Focal disruption of temporal cortex in macaque during midbrain-induced neglect

Amarender R. Bogadhi[1*], Anil Bollimunta[1], David A. Leopold[2,3], Richard J. Krauzlis[1*†]

1. Laboratory of Sensorimotor Research, National Eye Institute, National Institutes of Health

2. Laboratory of Neuropsychology, National Institute of Mental Health, National Institutes of Health

3. Neurophysiology Imaging Facility, National Institute of Mental Health, National Institute of Neurological Disorders and Stroke, National Eye Institute, National Institutes of Health

[†] Lead Contact

Correspondence:

bogadhi.amar@gmail.com

richard.krauzlis@nih.gov

Summary

Hemi-spatial neglect in humans is a common aftermath of stroke damage to subcortical and cortical brain structures, including the dorsocaudal temporal cortex. In macaques, reversible inactivation of some homologous brain structures (e.g. midbrain, prefrontal cortex) in selective attention tasks lead to behavioral symptoms of neglect, but as yet there is no evidence linking temporal cortex to neglect. To identify the neurological basis of neglect in macaques, we combined fMRI during attention tasks with pharmacologic suppression of midbrain activity. Functional mapping of brain areas during midbrain-induced neglect revealed a profound suppression of attention-related modulation in a small region (aFST/IPa) on the floor of the superior temporal sulcus. The same aFST/IPa region was also affected during neglect induced by inactivation of the prefrontal cortex. These results identify for the first time a region in the temporal cortex of macaque that is selectively affected during neglect induced by both subcortical and cortical inactivation.

Keywords: spatial neglect, selective attention, superior colliculus, temporal cortex, aFST/IPa region, fMRI, reversible inactivation, macaque

Introduction

In humans, hemi-spatial neglect is a common consequence of stroke damage to a range of cortical and subcortical structures (Corbetta and Shulman, 2011; Halligan et al., 2003; Heilman et al., 2000; Karnath and Rorden, 2012; Mesulam, 1981; Milner and McIntosh, 2005; Parton et al., 2004), and is defined as a behavioral syndrome characterized by failures to orient, detect or respond to stimuli in the visual field opposite to the brain lesion in the absence of sensory processing or motor deficits (Heilman et al., 1994; Rees et al., 2000). As such, hemi-spatial neglect is most closely associated with a disruption of attention-related mechanisms, that have been studied extensively in both humans and monkeys. Although neglect is diagnosed using clinical tests, performance deficits in attention-related paradigms such as the Posner cuing tasks are most sensitive during both acute and chronic stages (Rengachary et al., 2009).

The anatomy of spatial neglect is complex and entails the interaction between multiple brain systems. Spatial neglect is most commonly associated with damage to the inferior parietal and frontal cortices that have long been implicated in neglect (Bender and Butter, 1987; Critchley, 1953; Heilman and Valenstein, 1972; Husain and Kennard, 1996; Mort, 2003; Umarova et al., 2011; Verdon et al., 2010). At the same time, damage to subcortical structures in the telencephalon (e.g. striatum), thalamus (e.g. pulvinar) and midbrain (e.g. superior colliculus, SC) can lead to highly overlapping symptoms (Karnath et al., 2002; Snow et al., 2009; Weddell, 2004). Recent work in humans has placed emphasis on the temporal cortex, with meta-analysis suggesting that its contribution to spatial neglect has been previously under-appreciated (Karnath et

63 al., 2001). In particular, the dorsocaudal temporal cortex regions of the superior
64 temporal gyrus (STG) and temporo-parietal junction (TPJ) have been hypothesized to
65 play a particularly important role in spatial neglect (Chechlacz et al., 2010; Corbetta and
66 Shulman, 2002; Ellison, 2004; Friedrich et al., 1998; Hillis, 2005; Karnath, 2004; Meister
67 et al., 2006; Thiebaut de Schotten et al., 2005). These temporal cortical regions are also
68 part of the functional network with frontal and parietal areas implicated in spatial
69 attention in humans (Corbetta et al., 2005).

70 Understanding the brain mechanisms underlying spatial neglect requires
71 systematic testing of hypotheses in animal models such as the macaque, whose
72 perceptual specializations are similar to those in humans (Orban et al., 2004). Attention-
73 related deficits associated with visual neglect in humans have been demonstrated in the
74 macaque following reversible inactivation of several homologous brain structures, such
75 as the SC, pulvinar, parietal cortex (lateral intraparietal area, LIP) and prefrontal cortex
76 (frontal eye fields, FEF) (Gregoriou et al., 2014; Lovejoy and Krauzlis, 2010; Monosov et
77 al., 2011; Petersen et al., 1987; Wardak et al., 2004). However, the temporal cortical
78 regions functionally linked to spatial neglect are yet to be identified in monkeys (Patel et
79 al., 2015).

80 To determine brain regions functionally associated with spatial neglect in
81 monkeys, we performed fMRI before and during midbrain-induced neglect in two
82 monkeys performing visual selective attention tasks. We chose reversible inactivation of
83 midbrain SC to induce spatial neglect, because inactivation of this structure leads to
84 robust attention-related deficits, which are a hallmark of neglect (Lovejoy and Krauzlis,
85 2010; Zénon and Krauzlis, 2012). The broad coverage of fMRI provides a means to

compare attention-related modulation throughout the brain under normal behavior (“control”) and following SC inactivation (“neglect”) to identify brain regions functionally affected during the induced neglect phenomenon.

Our results show that, across the brain, the strongest unilateral suppression of attention-related modulation during midbrain-induced neglect was found in a circumscribed region (aFST/IPa) of the mid-STS cortex. Smaller unilateral reductions in modulation were observed in other regions of the cortex including FEF and part of area TPO. Surprisingly, neglect induced by inactivation of the prefrontal cortex also affected the same aFST/IPa region and additional experiments demonstrated that the reduction in attention-related modulation of the aFST/IPa region during neglect was not contingent on the stimulus feature used in the attention tasks. These findings identify for the first time a region in the mid-STS cortex of macaque that is linked to hemi-spatial neglect and is a functional component of both midbrain and prefrontal circuits associated with selective attention.

Results

Two adult macaques were scanned using BOLD fMRI across repeated sessions while performing three attention tasks. During some sessions, visual neglect was induced through inactivation of the superior colliculus using injection of muscimol, whereas during other sessions there was either no injection or the injection of a saline control. During fMRI data collection, the Baseline, Ignore and Attend tasks were presented in blocks (Fig. 1A-D; See Methods). In all three tasks, the color of the central cue indicated the relevant stimulus to be monitored for change detection. The monkeys maintained strict central fixation and reported the relevant changes detected by releasing a joystick. In Baseline task, monkeys monitored the fixation stimulus to detect a possible luminance change. The Ignore task was similar to the Baseline task but included peripheral visual stimuli that could change motion direction but were entirely task irrelevant. In the Attend task, monkeys monitored the same peripheral visual stimuli to detect possible changes in motion direction. Both monkeys performed the three attention tasks reliably, obtaining hit rates for relevant changes that were significantly higher than false alarm rates on both trials with task-irrelevant changes and catch trials containing no changes (Chi-square proportion test; $p<0.0001$).

Neglect induced by the suppression of midbrain activity

Spatial neglect was induced by reversible inactivation of the superior colliculus (SC). Specifically, we injected 0.3 – 0.5 μl of muscimol into the deep layers of SC (left SC in monkey #1 and right SC in monkey #2). In addition to the neglect effects, described below, inactivation affected the metrics of saccadic eye movements, including

126 changes in latency and peak eye velocity. These changes were a useful means to
127 monitor the location and duration of the muscimol effects on SC activity, as the saccadic
128 effects were retinotopic and affected only portions of the visual field (Fig. 1E). By
129 mapping the changes in saccade metrics caused by muscimol 30 minutes following the
130 end of injection, we were able to identify the specific portion of the visual field affected in
131 each session (blue region in Figure 1E) and confirm that the visual stimulus in the
132 attention tasks fully overlapped with the affected visual field (see Figure 1E, stimuli
133 depicted as white circles). Following the confirmation of SC inactivation, monkeys were
134 placed in the scanner for imaging in three attention tasks, which were always performed
135 while the animal maintained strict central fixation. The effectiveness of muscimol was
136 checked at the end of each imaging run (every 8 minutes) by having the monkeys
137 perform a pair of visually guided saccade into and out of the affected visual field
138 location, as illustrated for a sample session (Figure 1E, bottom); the difference in
139 latencies confirmed that the SC remained inactivated for the full duration of the imaging
140 runs in the experimental session. For every imaging session, the latencies of saccades
141 to targets into the affected field were significantly longer than the latencies of saccades
142 to targets in the unaffected visual field (Wilcoxon rank sum test; $p<0.05$).

143 Superior colliculus inactivation disrupted detection performance in the Attend
144 task for contralateral stimulus changes in both monkeys, in agreement with previous
145 findings (Lovejoy and Krauzlis, 2017; 2010; Zénon and Krauzlis, 2012). To quantify
146 these deficits, we compared the hit rate for motion-direction changes in the contralateral
147 visual field versus the ipsilateral visual field for each session (Fig. 1F). During SC
148 inactivation (blue symbols), all but one session showed a significant reduction in hit rate

149 for motion-direction changes for the stimulus in the affected contralateral visual field
150 compared to the stimulus in the unaffected ipsilateral visual field (Chi-square proportion
151 test; $p<0.05$). For the no-injection and saline sessions (orange and black symbols), we
152 did not find a significant difference in hit rates between the contralateral and ipsilateral
153 visual fields (Chi-square proportion test; $p<0.05$). These results show that SC
154 inactivation caused deficits in the detection of contralateral stimulus-change events,
155 akin to the deficits in the detection of contralateral targets observed in hemi-spatial
156 neglect (Corbetta et al., 2005; Rengachary et al., 2009). We refer to the deficits in the
157 Attend task during SC inactivation as *midbrain-induced neglect*.
158 Overall, we collected 18 sessions with muscimol injection (880 blocks each for
159 both the Ignore and Attend tasks in monkey #1, 912 blocks each for monkey #2), 16 no-
160 injection sessions (920 blocks each for both the Ignore and Attend tasks in monkey #1,
161 1008 blocks each for monkey #2), and 8 saline sessions in Monkey # 1 (928 blocks
162 each for both the Ignore and Attend tasks). Throughout the manuscript, we refer to the
163 no-injection sessions as “control” and the muscimol sessions as “neglect”.
164
165 *Midbrain-induced neglect linked to aFST/IPa region in the mid-STS cortex*
166 Taking advantage of the broad coverage of fMRI, we measured the attention-
167 related modulation of brain activity with and without midbrain-induced neglect.
168 Comparing these conditions allowed us to identify the brain regions that were selectively
169 affected during neglect. Attention-related modulation was defined as the contrast
170 between the Attend and Ignore tasks. To minimize the contribution of saccadic eye
171 movements, rewards and joystick-related movements, regressors for these variables

172 were included as part of the general linear model (see Methods). We further excluded
173 voxels that mapped onto foveal locations, based on a separate retinotopic mapping
174 experiment (see Methods), because these might be subject to the very small stimulus
175 differences at the fovea in the two conditions (black versus red cue; Fig. 1B, C). The
176 rationale for this approach and a full map of attention-related modulation including
177 foveal voxels in the same attention tasks and animals were described in a previous
178 study (Bogadhi et al., 2018).

179 In the absence of SC inactivation during control sessions, the Attend blocks
180 elicited higher BOLD responses in several brain areas compared to the Ignore blocks.
181 For each monkey, the t-score maps showing this attention-related modulation
182 (Bonferroni corrected; $p < 0.05$) were projected onto partially inflated cortical surface of
183 the hemisphere ipsilateral to the pending SC inactivation (Fig. 2A, 2C, see Fig. S1 for
184 contralateral hemispheres). Consistent with previous work (Caspari et al., 2015;
185 Stemmann and Freiwald, 2016), we found significant modulation in areas MT, MST,
186 FST, PGa, IPa and parts of TEO and TPO of the superior temporal sulcus, areas LIPd,
187 LIPv and area PEa of the intraparietal sulcus, and areas 45b, 8Bs, 8Ad, 8Av, 46d, 46v
188 of the frontal cortex (Fig. 2A, 2C).

189 Following midbrain-induced neglect, certain cortical subregions of the injected
190 hemisphere showed reduced attention-related modulation (Fig. 2B, 2D). In both
191 monkeys, the reduction was strongest in a portion of the mid-STS. In monkey #2 there
192 was no significant reduction in attention-related modulation outside of this region (Fig.
193 2D), whereas in monkey #1, weaker but statistically significant reductions were also
194 observed in IPS and frontal cortex (Fig. 2B). There was no evidence of suppressed

195 attention-related modulation in the contralateral hemisphere, although there was some
196 evidence of enhanced attention-related modulation (see Supplementary Fig. S1,
197 discussed further below).

198 To visualize the suppression in attention-related modulation across the cortex
199 during neglect, we performed a voxel-wise ANOVA with two factors and two levels each
200 – Covert attention (Attend and Ignore conditions) and Neglect (control and neglect
201 sessions). The ANOVA was based on the Attend and Ignore BOLD measurements in
202 the control and neglect sessions (see Methods), with the interaction term capturing the
203 attention-related deficits associated with neglect. This analysis was similar to the
204 ANOVA analysis used in a previous fMRI study in humans investigating the neural basis
205 and recovery of spatial attention deficits in neglect (Corbetta et al., 2005).

206 Hemi-neglect is characterized by behavioral deficits contralateral to injury or
207 inactivation of SC as demonstrated in this study (Fig. 1F). Thus, in the present
208 experiments, the cortical areas most directly linked to midbrain-induced neglect would
209 be ipsilateral to the injection site and show a unilateral suppression of BOLD attention-
210 related modulation during neglect. To identify the brain regions whose attention-related
211 modulation was suppressed unilaterally during neglect, we overlaid the interaction term
212 F-statistic from the voxel-wise ANOVA onto partially inflated cortical surfaces of the
213 ipsilateral hemispheres in both monkeys (Fig. 3A, 3B). The negative sign of the F-
214 statistic reflects decrease in modulation during neglect (see Methods).

215 The inflated maps of F-statistic in both monkeys show one contiguous patch of
216 blue in the mid-STS cortex (Fig. 3A, 3B). The blue region shows voxels strongly
217 affected in the aFST/IPa region during neglect (Monkey #1: F (1,24971) = -165.58;

218 Monkey #2: F (1, 26645) = -111.59). The degrees of freedom (Monkey #1: 24971;
219 Monkey #2: 26645) indicate the BOLD measurements during the Attend and Ignore
220 blocks across all the control and neglect sessions. A magnified view of the STS shows a
221 large swathe of blue in the mid-STS region that reflects the spatial extent of the
222 reduction in attention-related modulation during neglect (Fig. 3C, 3D). The affected
223 voxels in the mid-STS spanned two anatomical areas – anterior FST and posterior IPa
224 in both monkeys (Fig. 3C, 3D), and hence we refer to this region as aFST/IPa.
225 We localized the effect in aFST/IPa region to the lower part of the fundus in STS
226 in both monkeys at the same anterior-posterior location as shown in coronal slices (Fig.
227 3E, 3F). We observed a significant increase in modulation on the contralateral side
228 during neglect in both monkeys (Monkey #1: F (1,24971) = 29.83; Monkey #2: F (1,
229 26645) = 44.15). The unilateral suppression of modulation in the aFST/IPa region (Fig.
230 3E, 3F) combined with the lateralized behavioral deficits observed during neglect (Fig.
231 1F) demonstrates a strong link between aFST/IPa region and midbrain-induced neglect.
232 Control analyses accounting for other factors such as saccadic eye movements,
233 rewards, and joystick related movements (see Supplemental Info, Fig. S2), as well as
234 comparisons with saline injection controls (see Supplemental Info, Fig. S3) further
235 confirm and strengthen our finding that the aFST/IPa region in mid-STS cortex was
236 strongly linked to midbrain-induced neglect.
237
238 *Temporal and frontal cortical regions affected during midbrain-induced neglect*
239 The aFST/IPa region ipsilateral to SC inactivation was the most affected brain
240 region during neglect both in terms of size and spatial extent of the effect, and hence

241 pops out in the inflated maps of the voxel-wise analysis (blue region in Fig. 3). In
242 comparison, the effect in ipsilateral frontal cortex (Monkey #1: F (1,24971) = -38.07;
243 Monkey #2: F (1, 26645) = -40.51) and MT (Monkey #1: F (1,24971) = -33.71; Monkey
244 #2: F (1, 26645) = -50.87) was significant but weaker in spatial extent and size, and
245 hence was not easily seen in the inflated maps of the voxel-wise analysis (Fig. 3). To
246 quantify the effect on attention-related modulation during midbrain-induced neglect in
247 different cortical regions, we performed regions of interest (ROIs) analysis and identified
248 the brain regions that showed unilateral reduction in attention-related modulation,
249 consistent with the lateralized behavioral deficits observed during neglect (Fig. 1F).
250 Regions of interest (ROIs) were defined as 2mm-radius spheres centered on the
251 local maxima of the attention-related modulation map from the control sessions; we
252 compared the modulation in these ROIs between the control and neglect sessions.
253 Ipsilateral ROIs were defined based on the modulation maps shown in Fig. 2A, 2C and
254 contralateral ROIs were defined based on the modulation maps shown in Fig. S1A,
255 S1C. In total, we found 9 cortical ROIs that showed modulation at overlapping or
256 identical anatomical locations in both the ipsilateral and contralateral hemispheres of
257 both monkeys.
258 The 9 cortical ROIs for the hemisphere ipsilateral to the SC inactivation are
259 illustrated in Fig. 4. The coronal slices show the anatomical location and attention-
260 related modulation during control and neglect (as in Fig. 2), and the time-courses
261 quantify the %change in BOLD for Attend and Ignore conditions during control and
262 neglect. For each ROI, we also computed d-prime values (which capture effects on both
263 the mean and variance of the BOLD signal) to summarize the attention-related

264 modulation during control and neglect; the mean attention-related modulations (d') and
265 bootstrapped confidence intervals for both ipsilateral and contralateral ROIs during
266 control and neglect are shown in the bar plots (Fig. 4). To identify the regions with
267 significant changes, we then compared the modulation (d') during control and neglect
268 for ipsilateral and contralateral ROIs (bootstrap test; $p<0.05$). The rows in Fig. 4 present
269 the ROIs rank-ordered by the size of the unilateral effect on attention-related modulation
270 during midbrain-induced neglect.

271 Consistent with the voxel-wise ANOVA results (Fig. 3), we found significant
272 unilateral reductions in attention-related modulation across both monkeys in the
273 ipsilateral mid-STS ROIs – aFST/IPa and TPO (Fig. 4A, 4B). The effect was specific to
274 the hemisphere ipsilateral to SC inactivation – we did not find any reduction in
275 modulation of the contralateral aFST/IPa and TPO. On the contrary, we found an
276 increase in modulation of the contralateral aFST/IPa and TPO of monkey # 2, consistent
277 with the observation that monkey #2 showed a modest increase in performance (6.6 %)
278 for the ipsilateral stimulus in the Attend task (Fig. 1F). These results further strengthen
279 our finding that the mid-STS regions show unilateral suppression of modulation during
280 midbrain-induced neglect and highlight the strong link between mid-STS cortex and
281 neglect.

282 We also found regions with significant changes in the frontal and parietal cortex.
283 However, unilateral reduction in modulation was observed only in FEF. In the prefrontal
284 cortex, FEF showed significant reduction in modulation ipsilateral to SC inactivation in
285 both monkeys with no significant effect on the contralateral side (Fig. 4C). Another ROI
286 in the prefrontal cortex showed a significant effect only in one monkey: there was a

287 significant reduction in modulation of ipsilateral and contralateral vlPFC in monkey #1
288 but not in monkey #2 (Fig. 4D). In the parietal cortex, we found significant reduction in
289 ipsilateral LIPd of both monkeys and contralateral LIPd of monkey #2 (Fig. 4E). In
290 monkey #2, both ipsilateral and contralateral effects in LIPd were of equal magnitude,
291 with no significant effect in LIPv (Fig. 4F).

292 There were also some changes in visual areas but the effects were not unilateral
293 and were mixed across both monkeys. In ipsilateral MT, both monkeys showed
294 significant reduction in modulation (Fig. 4G). However, we also found a significant but
295 modest reduction in contralateral MT that was smaller compared to the reduction in
296 ipsilateral MT. In V2v, both monkeys showed significant reductions in the ipsilateral
297 ROI. However, Monkey #1 also showed a significant and larger reduction in
298 contralateral V2v (Fig. 4H). In visual cortical ROI V1, we found a significant reduction in
299 modulation ipsilateral to SC inactivation in one monkey (Fig. 4I).

300 Control analyses comparing attention-related modulation in different ROIs during
301 neglect and saline sessions (see Supplemental Info, Fig. S4) further confirm that the
302 temporal cortical regions – aFST/IPa and TPO, along with FEF in the prefrontal cortex
303 showed a unilateral reduction in modulation during midbrain-induced neglect. We also
304 verified that these findings were robust to the attention-related measure (d') we used by
305 computing another attention-related measure that is equivalent to the β coefficient of the
306 term contrasting Attend and Ignore conditions – namely, the difference between mean
307 BOLD in Attend and mean BOLD in Ignore ($\mu_A - \mu_I$). These findings taken together with
308 the results from the voxel-wise analysis implicate for the first time a region in the

309 macaque temporal cortex in visual hemi-neglect, in this case induced through
310 inactivation of the SC.
311
312 *Effect in aFST/IPa region during neglect was not contingent on visual motion*
313 A possible explanation for the reduction of attention-related modulation in the
314 aFST/IPa region of macaque temporal cortex during midbrain-induced neglect is that
315 the aFST/IPa region is related to higher-order motion processing. This explanation is
316 partially consistent with previous fMRI reports showing activations related to higher-
317 order motion processing and object-related processing in similar parts of the mid-STS
318 cortex (Nelissen et al., 2006). To test if the effect in the aFST/IPa region during neglect
319 was contingent on visual motion, we performed fMRI in similar attention tasks with and
320 without SC inactivation in monkey #1 using a non-motion stimulus. All the attention
321 tasks were the same as before, except that the motion stimuli were replaced with white
322 noise stimuli and motion-change detection was replaced with a second-order orientation
323 detection (see Methods). In the Ignore task, the monkey monitored the fixation stimulus
324 for a luminance-change and ignored the peripheral white noise distractor stimuli and the
325 brief second-order (i.e., defined by contrast not luminance) orientation pulse (Fig. 5A).
326 In the Attend task, the monkey monitored the peripheral white noise stimuli and
327 detected the brief second-order orientation pulse (Fig. 5B). The SC inactivation and
328 other methods were the same as described for the motion stimuli experiments (Fig. 1).
329 We confirmed that SC inactivation significantly affected performance for the
330 contralateral second-order orientation changes compared to the ipsilateral second-order
331 orientation changes in the Attend task during all sessions (Fig. 5C; Chi-square

332 proportion test; $p<0.05$). We collected 7 no-injection (824 blocks each for both the
333 Ignore and Attend tasks) and 9 SC inactivation sessions (848 blocks each for both the
334 Ignore and Attend tasks) which we refer to as control and midbrain-induced neglect
335 sessions, respectively.

336 First, we determined if the aFST/IPa region showed attention-related modulation
337 in the absence of visual motion by contrasting Attend and Ignore tasks in the control
338 sessions (Bonferroni corrected; $p<0.05$). We found significant attention-related
339 modulation in the aFST/IPa region (see black arrow in Fig. 5D), in addition to areas of
340 posterior STS, IPS and the frontal cortex. The attention-related modulation in the
341 second-order orientation task was sparser compared to that in the motion-change
342 detection task, perhaps because the orientation stimulus lacked the continuous dynamic
343 changes of the motion stimulus. These results show that the aFST/IPa region was
344 modulated during covert visual attention even in the absence of visual motion.

345 Second, we determined if the attention-related modulation in aFST/IPa during the
346 second-order orientation task was also changed during midbrain-induced neglect (Fig.
347 5E), using the same voxel-wise ANOVA analysis described in the earlier section. The
348 inflated map of the interaction term F-statistic in the ipsilateral STS of monkey #1
349 showed that the voxels most affected during neglect were once again identified in the
350 mid-STS region at the border between anterior FST and posterior IPa ($F(1, 23083) = -$
351 63.64; see white arrow in Fig. 5F). On the contrary, there was no effect in the
352 contralateral mid-STS region during neglect ($F(1, 23083) = 0.000419$). Importantly, the
353 affected voxels in the mid-STS (blue region in Fig. 5F) completely overlapped with the
354 aFST/IPa region that was affected in the motion task (white contour in Fig. 5F). In fact,

355 further localization of the affected voxels revealed the same lower part of the fundus in
356 STS at the identical anterior-posterior location (compare Fig. 5G and Fig. 3E). These
357 results show that the same voxels in the aFST/IPa region were affected during neglect
358 in both the motion and second-order orientation tasks, demonstrating that the effect in
359 aFST/IPa region during midbrain-induced neglect was not contingent on visual motion.
360

361 *The same aFST/IPa region was affected during neglect induced by FEF inactivation*

362 Is the selective involvement of the aFST/IPa region specific for midbrain-induced
363 neglect, or would cortically induced neglect similarly reduce attention-related modulation
364 in this mid-STS region? To address this, we inactivated the frontal eye fields (FEF) of
365 the prefrontal cortex in separate experiments. Like the SC, FEF inactivation in
366 macaques has previously been shown to lead to performance deficits akin to spatial
367 neglect (Gregoriou et al., 2014; Monosov et al., 2011). We identified FEF in the anterior
368 bank of the arcuate sulcus using microstimulation with currents of 40 μA to evoke
369 saccades (Fig. 6A). For reversible inactivation, we injected 1-2 μl of muscimol and
370 mapped the affected visual field using a visually guided saccade task (see Methods;
371 Fig. 6B). The contralateral stimulus in the attention task (white circle) fully overlapped
372 the portion of the visual field showing saccade deficits during FEF inactivation (blue
373 region). We also confirmed that the muscimol effect lasted throughout the entire
374 imaging session using the same methodology as described for SC inactivation and
375 imaging (see Methods).

376 Perceptual choices in the Attend task for contralateral motion-changes compared
377 to ipsilateral motion-changes were not significantly affected during FEF inactivation.

378 However, we did find a significant effect on the median response times for contralateral
379 motion-changes compared to ipsilateral motion-changes (median RT_{contra} = 545 ms;
380 RT_{ipsi} = 521 ms; Wilcoxon rank sum test; $p<0.001$). A similar comparison of median
381 response times during control sessions did not show any significant effect (median
382 RT_{contra} = 523 ms; RT_{ipsi} = 523 ms; Wilcoxon rank sum test; $p=0.92$). These results
383 confirmed that prefrontal cortex causally affects performance in attention tasks akin to
384 spatial neglect. Over all, we collected 7 no-injection (768 blocks each for both the Ignore
385 and Attend tasks) and 7 inactivation sessions (736 blocks each for both the Ignore and
386 Attend tasks), which we refer to as control and FEF-induced neglect sessions,
387 respectively.

388 Before determining if aFST/IPa region was affected during FEF-induced neglect,
389 we confirmed that the aFST/IPa region (see black arrow in Fig. 6C) showed significant
390 attention-related modulation during control sessions in addition to other regions of STS,
391 IPS, AS and PS (Fig. 6C), in agreement with the attention-related modulations observed
392 previously in the same task (Fig. 2C). To determine the effect of FEF-induced neglect
393 on the attention-related modulation throughout cortex (Fig. 6D), we performed the same
394 voxel-wise ANOVA analysis as described in earlier section and the F-statistic of the
395 interaction term for voxels in the ipsilateral STS is shown on the inflated cortical surface
396 in Fig. 6D.

397 The voxels most affected during FEF-induced neglect were again found in the
398 ipsilateral mid-STS region at the border between anterior FST and IPa ($F(1, 21322) = -$
399 93; white arrow in Fig. 6E), with no significant effect in the contralateral mid-STS region
400 ($F(1, 21322) = 2.684$). The affected region during FEF-induced neglect (blue region)

401 fully overlapped with the affected region during midbrain-induced neglect (white
402 contour). Further localization showed the affected region to be in the fundus of STS at a
403 similar anterior-posterior location (compare Fig. 6F and Fig. 3F). These results show
404 that the aFST/IPa region was affected not only during midbrain-induced neglect but also
405 during neglect induced by FEF inactivation.

406 The effect in aFST/IPa region during FEF inactivation was weaker compared to
407 the effect in aFST/IPa during SC inactivation (compare Fig. 3D and Fig. 6E). We
408 suspect this was likely because of the difference in performance deficits in the attention
409 tasks during FEF and SC inactivations. SC inactivation resulted in significant
410 performance deficits whereas FEF inactivation yielded modest but significant reaction
411 time effects. A stronger inactivation of FEF with a higher volume of muscimol might
412 have yielded comparable deficits to SC inactivation. Regardless of the size of the effect
413 in aFST/IPa during FEF inactivation, our results show that the aFST/IPa region was
414 affected during neglect induced by both cortical and subcortical inactivation.
415
416
417
418

Discussion

In humans, the anatomy of hemi-spatial neglect includes regions of the superior temporal cortex that are part of a network with frontal and parietal cortex and subcortical brain structures (Corbetta et al., 2005; Hillis, 2005; Karnath et al., 2005). However, temporal cortical regions linked to spatial neglect have not yet been identified in monkeys. In this study, we combined fMRI with and without hemi-spatial neglect induced by reversible inactivation of superior colliculus in monkeys performing a covert attention task and identified the strongest reduction in attention-related modulation during midbrain-induced neglect in the temporal cortex. Specifically, a contiguous cluster of voxels in the ipsilateral aFST/IPa region of the mid-STS showed a dramatic reduction in attention-related modulation during neglect, and this effect was not contingent on stimulus motion. Moreover, this reduction was accompanied by a modest but significant increase in the contralateral aFST/IPa region. In comparison, smaller unilateral reductions in modulation were observed in other ipsilateral regions of the cortex including FEF and part of area TPO. These findings, taken together with the performance deficits during neglect, demonstrate for the first time in monkeys a strong link between modulation in the mid-STS region of the temporal cortex and attention-related deficits associated with neglect.

Possible pathways from superior colliculus to mid-STS cortex

How does suppression of activity in superior colliculus have such a profound influence on the modulation in the aFST/IPa region of the mid-STS cortex? Among several tectofugal pathways (Benevento and Fallon, 1975; Partlow et al., 1977), we

442 speculate two possible pathways through thalamus as the likely candidates for
443 mediating these effects. The first is the pathway from the intermediate and deep layers
444 of SC to medial pulvinar and the reciprocal connections between medial pulvinar and
445 regions of the mid-STS cortex (Benevento and Standage, 1983; Burton and Jones,
446 1976; Yeterian and Pandya, 1989). The second is the pathway from the intermediate
447 and deep layers of SC to FEF through mediodorsal thalamus (Benevento and Fallon,
448 1975), and FEF projections to regions of the mid-STS cortex (Stanton et al., 1995). The
449 dramatic reduction in modulation in the aFST/IPa region compared to the FEF during
450 midbrain-induced neglect suggests that the pathway through the medial pulvinar might
451 have larger influence on the aFST/IPa region compared to the pathway through FEF.
452
453 *Priority maps in the subcortical and cortical areas causally affect the aFST/IPa region*
454 Superior colliculus activity represents spatial "priority maps" and suppression of
455 this activity leads to robust performance deficits in attention tasks akin to neglect
456 (Fecteau and Munoz, 2006; Lovejoy and Krauzlis, 2010). In addition to the SC,
457 prefrontal cortex (FEF) is another brain structure that represents spatial "priority maps"
458 and suppression of activity in FEF also leads to performance deficits akin to spatial
459 neglect (Gregoriou et al., 2014; Monosov et al., 2011). Our results showed that
460 attention-related BOLD modulation in the same aFST/IPa region was reduced when
461 activity in SC or FEF was suppressed, demonstrating that these subcortical and cortical
462 "priority maps" causally influence the aFST/IPa region. This finding is in agreement with
463 previous fMRI reports that similar mid-STS regions are causally affected by
464 manipulations in frontal and parietal areas FEF and LIP (Ekstrom et al., 2008; Wilke et

465 al., 2012). In addition, these mid-STS regions are reciprocally connected with the dorsal
466 and ventral stream areas. These results taken together with previous anatomical
467 evidence suggest that the mid-STS regions (aFST/IPa and TPO) may combine spatial
468 "priority maps" from the sensorimotor structures (SC, FEF, LIP) with the visual
469 information from the dorsal and ventral stream areas (Boussaoud et al., 1990; Saleem
470 et al., 2000).
471
472 *aFST/IPa region: a potential homolog of the human temporoparietal junction?*
473 In humans, temporal cortical regions including the temporoparietal junction (TPJ)
474 and its neighboring superior temporal cortical areas play a crucial role in spatial neglect
475 (Corbetta and Shulman, 2011; Karnath and Rorden, 2012), and are functionally
476 connected to frontal and parietal areas (Corbetta et al., 2005). In macaques, similar
477 mid-STS regions as identified in this study are functionally connected to the
478 sensorimotor structures (SC, FEF, LIP) implicated in spatial attention and neglect
479 (Ekstrom et al., 2008; Wilke et al., 2012). This functional dependence on sensorimotor
480 structures raises an interesting possibility that these mid-STS regions in macaque are
481 homologous to the areas of the superior temporal cortex associated with spatial neglect
482 in the human. At the same time, a recent study comparing humans and monkeys in an
483 attention task was unable to identify a functional homologue of TPJ in the macaque, and
484 thus concluded the opposite – that the human TPJ likely evolved independently and is
485 not a shared primate feature (Patel et al., 2015). Importantly, the authors suggested that
486 the macaque might not be an adequate animal model to study mechanisms of spatial
487 attention and neglect. Here, by demonstrating a prominent and focal area in the mid-

488 STS region that is affected during neglect induced by both cortical and subcortical
489 inactivation, our findings suggest the TPJ region in humans has a potential homologue
490 in the macaques. Beyond the location in the temporal cortex, the causal dependence of
491 the mid-STS region on activity in sensorimotor spatial “priority maps” (SC, FEF) is
492 similar to the proposed link between temporal cortical regions of the ventral attention
493 network and sensorimotor areas of the dorsal attention network in human neglect
494 (Corbetta and Shulman, 2011). While homology is notoriously difficult to establish, these
495 findings for the first time establish a functional link between the temporal cortex and
496 hemi-spatial neglect in the macaque and offers a new bridge between human and
497 nonhuman primate models of hemi-spatial neglect.
498
499 *aFST/IPa region could be polysensory and may play a role in target detection*
500 As far as we know, there is no electrophysiology data available to infer function
501 from the properties of neurons in the aFST/IPa region we identified, although there is
502 fMRI evidence that similar parts of the STS show motion-sensitivity as well as object-
503 selectivity (Nelissen et al., 2006). Inspection of the electrophysiology literature for the
504 neighboring cortical areas suggests that the aFST/IPa region closely corresponds to the
505 middle part of the superior temporal polysensory (STP) region (Scalaidhe et al., 1995),
506 and visual activity of neurons in the STP region depend on striate cortex and midbrain
507 SC (Bruce et al., 1986). These previous findings taken together with our result that
508 modulation in aFST/IPa region depends on midbrain activity suggest that the aFST/IPa
509 region is likely to be a part of the STP region. Neurons in the caudal and rostral parts of
510 the STP region respond to visual, auditory and somesthetic stimuli and exhibit not only

511 unimodal but also bimodal and trimodal response properties (Bruce et al., 1981;
512 Hikosaka et al., 1988). Neurons in the anterior (rostral) STP region are also selective for
513 3D structure from motion (Anderson and Siegel, 2005), similar to neurons in the middle
514 part of area FST (Mysore et al., 2010). Importantly, STP lesions result in delayed
515 detection of contralateral targets (Scalaidhe et al., 1995), and lesions in the dorsal bank
516 and fundus of STS result in unilateral neglect (Luh et al., 1986; Watson et al., 1994).
517 These observations from the overlapping and neighboring regions suggest that the
518 aFST/IPa region is likely part of the previously described STP region that contains cells
519 responsive to multi-modal stimulation and may play a role in target detection.
520

521 *Conclusion*

522 Using fMRI and reversible inactivation in monkeys performing attention tasks, we
523 identified a novel brain region in the mid-STS cortex (aFST/IPa) to be the most affected
524 brain region during neglect induced by subcortical and cortical inactivation, and we
525 showed that this effect is not contingent on the specific visual feature used in the
526 attention tasks. Our results demonstrate for the first time in monkeys a functional link
527 between temporal cortex and neglect, thereby bridging the gap between human and
528 macaque model of hemi-spatial neglect. Future experiments in the aFST/IPa region
529 should address the neuronal responses and their modulation, at different epochs in the
530 selective attention tasks, both before and during neglect, to better understand the
531 functional link between aFST/IPa neuronal activity and neglect. Such experiments might
532 also provide insights into why loss of activity from the midbrain SC, an evolutionarily
533 ancient structure important for orienting movements, appears to especially affect this

534 particular region of primate visual cortex, amongst the many neocortical areas that
535 could have been affected.
536
537 **Acknowledgments**
538 We thank Tom Ruffner and Nick Nichols for technical support and Fabrice
539 Arcizet, James Herman, Leor Katz and Lupeng Wang for helpful input. We also thank
540 Brian Russ for helpful suggestions in setting up fMRI preprocessing pipeline and
541 constructing inflated maps. This work was supported by the National Eye Institute
542 Intramural Research Program at the National Institutes of Health. Functional and
543 anatomical MRI scanning was carried out in the Neurophysiology Imaging Facility Core
544 (NIMH, NINDS, NEI) supported under IRP grant ZIC MH002899. This work utilized the
545 computational resources of the NIH HPC Biowulf cluster.
546
547 **Author Contributions**
548 All authors designed the experiments. A.R.B. and A.B. conducted experiments and
549 collected the data. A.R.B. analyzed the data. All authors interpreted the results. A.R.B.
550 and R.J.K wrote the manuscript.
551
552 **Declaration of interests:** The authors declare no competing interests.
553

References

Anderson, K.C., Siegel, R.M., 2005. Three-dimensional structure-from-motion selectivity in the anterior superior temporal polysensory area, STPa, of the behaving monkey. Cereb. Cortex 15, 1299–1307. doi:10.1093/cercor/bhi013

Bender, D.B., Butter, C.M., 1987. Comparison of the effects of superior colliculus and pulvinar lesions on visual search and tachistoscopic pattern discrimination in monkeys. Exp Brain Res 69, 140–154. doi:10.1007/BF00247037

Benevento, L.A., Fallon, J.H., 1975. The ascending projections of the superior colliculus in the rhesus monkey (Macaca mulatta). J. Comp. Neurol. 160, 339–361. doi:10.1002/cne.901600306

Benevento, L.A., Standage, G.P., 1983. The organization of projections of the retinorecipient and nonretinorecipient nuclei of the pretectal complex and layers of the superior colliculus to the lateral pulvinar …. Journal of Comparative ….

Bogadhi, A.R., Bollimunta, A., Leopold, D.A., Krauzlis, R.J., 2018. Brain regions modulated during covert visual attention in the macaque. bioRxiv. doi:10.1101/340703

Boussaoud, D., Ungerleider, L.G., Desimone, R., 1990. Pathways for motion analysis: cortical connections of the medial superior temporal and fundus of the superior temporal visual areas in the macaque. J. Comp. Neurol. 296, 462–495. doi:10.1002/cne.902960311

Brainard, D.H., 1997. The Psychophysics Toolbox. Spat Vis 10, 433–436.

Bruce, C., Desimone, R., Gross, C.G., 1981. Visual properties of neurons in a polysensory area in superior temporal sulcus of the macaque. Journal of

577 Neurophysiology 46, 369–384.
578 Bruce, C.J., Desimone, R., Gross, C.G., 1986. Both striate cortex and superior colliculus
579 contribute to visual properties of neurons in superior temporal polysensory area of
580 macaque monkey. Journal of Neurophysiology 55, 1057–1075.
581 Bruce, C.J., Goldberg, M.E., 1985. Primate frontal eye fields. I. Single neurons
582 discharging before saccades. Journal of Neurophysiology 53, 603–635.
583 doi:10.1152/jn.1985.53.3.603
584 Burton, H., Jones, E.G., 1976. The posterior thalamic region and its cortical projection in
585 New World and Old World monkeys. J. Comp. Neurol. 168, 249–301.
586 doi:10.1002/cne.901680204
587 Caspari, N., Janssens, T., Mantini, D., Vandenberghe, R., Vanduffel, W., 2015. Covert
588 Shifts of Spatial Attention in the Macaque Monkey. Journal of Neuroscience 35,
589 7695–7714. doi:10.1523/JNEUROSCI.4383-14.2015
590 Chechlacz, M., Rotshtein, P., Bickerton, W.-L., Hansen, P.C., Deb, S., Humphreys,
591 G.W., 2010. Separating neural correlates of allocentric and egocentric neglect:
592 Distinct cortical sites and common white matter disconnections. Cognitive
593 Neuropsychology 27, 277–303. doi:10.1080/02643294.2010.519699
594 Chen, L.L., Goffart, L., Sparks, D.L., 2001. A simple method for constructing
595 microinjectrodes for reversible inactivation in behaving monkeys. J. Neurosci.
596 Methods 107, 81–85.
597 Corbetta, M., Kincade, M.J., Lewis, C., Snyder, A.Z., Sapir, A., 2005. Neural basis and
598 recovery of spatial attention deficits in spatial neglect. Nat. Neurosci. 8, 1603–1610.
599 doi:10.1038/nn1574

600 Corbetta, M., Shulman, G.L., 2011. Spatial Neglect and Attention Networks. Annu. Rev.
601 Neurosci. 34, 569–599. doi:10.1146/annurev-neuro-061010-113731
602 Corbetta, M., Shulman, G.L., 2002. CONTROL OF GOAL-DIRECTED AND STIMULUS-
603 DRIVEN ATTENTION IN THE BRAIN. Nature Reviews Neuroscience 3, 215–229.
604 doi:10.1038/nrn755
605 Cox, R.W., 1996. AFNI: software for analysis and visualization of functional magnetic
606 resonance neuroimages. Comput. Biomed. Res. 29, 162–173.
607 Critchley, M., 1953. The Parietal Lobes.
608 Eastman, K.M., Huk, A.C., 2012. PLDAPS: A Hardware Architecture and Software
609 Toolbox for Neurophysiology Requiring Complex Visual Stimuli and Online
610 Behavioral Control. Front Neuroinform 6, 1. doi:10.3389/fninf.2012.00001
611 Ekstrom, L.B., Roelfsema, P.R., Arsenault, J.T., Bonmassar, G., Vanduffel, W., 2008.
612 Bottom-up dependent gating of frontal signals in early visual cortex. Science 321,
613 414–417. doi:10.1126/science.1153276
614 Ellison, A., 2004. An exploration of the role of the superior temporal gyrus in visual
615 search and spatial perception using TMS. Brain 127, 2307–2315.
616 doi:10.1093/brain/awh244
617 Fecteau, J.H., Munoz, D.P., 2006. Salience, relevance, and firing: a priority map for
618 target selection. Trends Cogn. Sci. (Regul. Ed.) 10, 382–390.
619 doi:10.1016/j.tics.2006.06.011
620 Friedrich, F.J., Egly, R., Rafal, R.D., Beck, D., 1998. Spatial attention deficits in
621 humans: a comparison of superior parietal and temporal-parietal junction lesions.
622 Neuropsychology 12, 193–207.

623 Gregoriou, G.G., Rossi, A.F., Ungerleider, L.G., Desimone, R., 2014. Lesions of
624 prefrontal cortex reduce attentional modulation of neuronal responses and
625 synchrony in V4. Nat. Neurosci. 17, 1003–1011. doi:10.1038/nn.3742
626 Halligan, P.W., Fink, G.R., Marshall, J.C., Vallar, G., 2003. Spatial cognition: evidence
627 from visual neglect. Trends Cogn. Sci. (Regul. Ed.) 7, 125–133. doi:10.1016/S1364-
628 6613(03)00032-9
629 Heilman, K.M., Valenstein, E., 1972. Frontal lobe neglect in man. Neurology 22, 660–
630 664.
631 Heilman, K.M., Valenstein, E., Watson, R.T., 2000. Neglect and related disorders.
632 Semin Neurol 20, 463–470. doi:10.1055/s-2000-13179
633 Heilman, K.M., Valenstein, E., Watson, R.T., 1994. The what and how of neglect.
634 Neuropsychological Rehabilitation 4, 133–139. doi:10.1080/09602019408402270
635 Hikosaka, K., Iwai, E., Saito, H., Tanaka, K., 1988. Polysensory properties of neurons in
636 the anterior bank of the caudal superior temporal sulcus of the macaque monkey.
637 Journal of Neurophysiology 60, 1615–1637.
638 Hillis, A.E., 2005. Anatomy of Spatial Attention: Insights from Perfusion Imaging and
639 Hemispatial Neglect in Acute Stroke. Journal of Neuroscience 25, 3161–3167.
640 doi:10.1523/JNEUROSCI.4468-04.2005
641 Husain, M., Kennard, C., 1996. Visual neglect associated with frontal lobe infarction. J.
642 Neurol. 243, 652–657.
643 Karnath, H.-O., Rorden, C., 2012. The anatomy of spatial neglect. Neuropsychologia
644 50, 1010–1017. doi:10.1016/j.neuropsychologia.2011.06.027
645 Karnath, H.-O., Zopf, R., Johannsen, L., Berger, M.F., Nägele, T., Klose, U., 2005.

646 Normalized perfusion MRI to identify common areas of dysfunction: patients with
647 basal ganglia neglect. Brain 128, 2462–2469. doi:10.1093/brain/awh629
648 Karnath, H.O., 2004. The Anatomy of Spatial Neglect based on Voxelwise Statistical
649 Analysis: A Study of 140 Patients. Cereb. Cortex 14, 1164–1172.
650 doi:10.1093/cercor/bhh076
651 Karnath, H.O., Ferber, S., Himmelbach, M., 2001. Spatial awareness is a function of the
652 temporal not the posterior parietal lobe. Nature 411, 950–953.
653 doi:10.1038/35082075
654 Karnath, H.O., Himmelbach, M., Rorden, C., 2002. The subcortical anatomy of human
655 spatial neglect: putamen, caudate nucleus and pulvinar. Brain.
656 Kleiner, M., Brainard, D., Pelli, D., 2007. What's new in Psychtoolbox-3? Perception 36.
657 Lovejoy, L.P., Krauzlis, R.J., 2017. Changes in perceptual sensitivity related to spatial
658 cues depends on subcortical activity. PNAS 114, 6122–6126.
659 doi:10.1073/pnas.1609711114
660 Lovejoy, L.P., Krauzlis, R.J., 2010. Inactivation of primate superior colliculus impairs
661 covert selection of signals for perceptual judgments. Nat. Neurosci. 13, 261–266.
662 doi:10.1038/nn.2470
663 Luh, K.E., Butter, C.M., Buchtel, H.A., 1986. Impairments in orienting to visual stimuli in
664 monkeys following unilateral lesions of the superior sulcal polysensory cortex.
665 Neuropsychologia 24, 461–470. doi:10.1016/0028-3932(86)90091-6
666 Madelain, L., Krauzlis, R.J., Wallman, J., 2005. Spatial deployment of attention
667 influences both saccadic and pursuit tracking. Vision Research 45, 2685–2703.
668 doi:10.1016/j.visres.2005.05.009

669 Meister, I.G., Wienemann, M., Buelte, D., Grünewald, C., Sparing, R., Dambeck, N.,
670 Boroojerdi, B., 2006. Hemiextinction induced by transcranial magnetic stimulation
671 over the right temporo-parietal junction. Neuroscience 142, 119–123.
672 doi:10.1016/j.neuroscience.2006.06.023
673 Mesulam, M.M., 1981. A cortical network for directed attention and unilateral neglect.
674 Ann. Neurol. 10, 309–325. doi:10.1002/ana.410100402
675 Milner, A.D., McIntosh, R.D., 2005. The neurological basis of visual neglect. Curr. Opin.
676 Neurol. 18, 748–753.
677 Monosov, I.E., Sheinberg, D.L., Thompson, K.G., 2011. The effects of prefrontal cortex
678 inactivation on object responses of single neurons in the inferotemporal cortex
679 during visual search. J. Neurosci. 31, 15956–15961.
680 doi:10.1523/JNEUROSCI.2995-11.2011
681 Mort, D.J., 2003. The anatomy of visual neglect. Brain 126, 1986–1997.
682 doi:10.1093/brain/awg200
683 Mysore, S.G., Vogels, R., Raiguel, S.E., Todd, J.T., Orban, G.A., 2010. The selectivity
684 of neurons in the macaque fundus of the superior temporal area for three-
685 dimensional structure from motion. J. Neurosci. 30, 15491–15508.
686 doi:10.1523/JNEUROSCI.0820-10.2010
687 Nelissen, K., Vanduffel, W., Orban, G.A., 2006. Charting the lower superior temporal
688 region, a new motion-sensitive region in monkey superior temporal sulcus. J.
689 Neurosci. 26, 5929–5947. doi:10.1523/JNEUROSCI.0824-06.2006
690 Orban, G.A., Van Essen, D., Vanduffel, W., 2004. Comparative mapping of higher visual
691 areas in monkeys and humans. Trends Cogn. Sci. (Regul. Ed.) 8, 315–324.

692 doi:10.1016/j.tics.2004.05.009
693 Partlow, G.D., Colonnier, M., Szabo, J., 1977. Thalamic projections of the superior
694 colliculus in the rhesus monkey, Macaca mulatta. A light and electron microscopic
695 study. J. Comp. Neurol. 72, 285–318.
696 Parton, A., Malhotra, P., Husain, M., 2004. Hemispatial neglect. J Neurol Neurosurg
697 Psychiatry 75, 13–21.
698 Patel, G.H., Yang, D., Jamerson, E.C., Snyder, L.H., Corbetta, M., Ferrera, V.P., 2015.
699 Functional evolution of new and expanded attention networks in humans. PNAS
700 201420395. doi:10.1073/pnas.1420395112
701 Pelli, D.G., 1997. The VideoToolbox software for visual psychophysics: transforming
702 numbers into movies. Spat Vis 10, 437–442.
703 Petersen, S.E., Robinson, D.L., Morris, J.D., 1987. Contributions of the pulvinar to
704 visual spatial attention. Neuropsychologia 25, 97–105. doi:10.1016/0028-
705 3932(87)90046-7
706 Rees, G., Wojciulik, E., Clarke, K., Husain, M., Frith, C., Driver, J., 2000. Unconscious
707 activation of visual cortex in the damaged right hemisphere of a parietal patient with
708 extinction. Brain 123 (Pt 8), 1624–1633.
709 Rengachary, J., d'Avossa, G., Sapir, A., Shulman, G.L., Corbetta, M., 2009. Is the
710 Posner Reaction Time Test More Accurate Than Clinical Tests in Detecting Left
711 Neglect in Acute and Chronic Stroke? YAPMR 90, 2081–2088.
712 doi:10.1016/j.apmr.2009.07.014
713 Reveley, C., Gruslys, A., Ye, F.Q., Glen, D., Samaha, J., E Russ, B., Saad, Z., K Seth,
714 A., Leopold, D.A., Saleem, K.S., 2017. Three-Dimensional Digital Template Atlas of

715 the Macaque Brain. Cereb. Cortex 27, 4463–4477. doi:10.1093/cercor/bhw248
716 Robinson, D.A., 1972. Eye movements evoked by collicular stimulation in the alert
717 monkey. Vision Research 12, 1795–1808.
718 Saleem, K.S., Suzuki, W., Tanaka, K., Hashikawa, T., 2000. Connections between
719 anterior inferotemporal cortex and superior temporal sulcus regions in the macaque
720 monkey. J. Neurosci. 20, 5083–5101.
721 Scalaidhe, S.P., Albright, T.D., Rodman, H.R., Gross, C.G., 1995. Effects of superior
722 temporal polysensory area lesions on eye movements in the macaque monkey.
723 Journal of Neurophysiology 73, 1–19.
724 Snow, J.C., Allen, H.A., Rafal, R.D., Humphreys, G.W., 2009. Impaired attentional
725 selection following lesions to human pulvinar: Evidence for homology between
726 human and monkey. PNAS 106, 4054–4059. doi:10.1073/pnas.0810086106
727 Stanton, G.B., Bruce, C.J., Goldberg, M.E., 1995. Topography of projections to posterior
728 cortical areas from the macaque frontal eye fields. J. Comp. Neurol. 353, 291–305.
729 doi:10.1002/cne.903530210
730 Stemmann, H., Freiwald, W.A., 2016. Attentive Motion Discrimination Recruits an Area
731 in Inferotemporal Cortex. J. Neurosci. 36, 11918–11928.
732 doi:10.1523/JNEUROSCI.1888-16.2016
733 Thiebaut de Schotten, M., Urbanski, M., Duffau, H., Volle, E., Lévy, R., Dubois, B.,
734 Bartolomeo, P., 2005. Direct evidence for a parietal-frontal pathway subserving
735 spatial awareness in humans. Science 309, 2226–2228.
736 doi:10.1126/science.1116251
737 Umarova, R.M., Saur, D., Kaller, C.P., Vry, M.-S., Glauche, V., Mader, I., Hennig, J.,

738 Weiller, C., 2011. Acute visual neglect and extinction: distinct functional state of the
739 visuospatial attention system. Brain 134, 3310–3325. doi:10.1093/brain/awr220
740 Van Essen, D.C., Drury, H.A., Dickson, J., Harwell, J., Hanlon, D., Anderson, C.H.,
741 2001. An integrated software suite for surface-based analyses of cerebral cortex. J
742 Am Med Inform Assoc 8, 443–459.
743 Verdon, V., Schwartz, S., Lovblad, K.O., Hauert, C.A., Vuilleumier, P., 2010.
744 Neuroanatomy of hemispatial neglect and its functional components: a study using
745 voxel-based lesion-symptom mapping. Brain 133, 880–894.
746 doi:10.1093/brain/awp305
747 Wardak, C., Olivier, E., Duhamel, J.-R., 2004. A deficit in covert attention after parietal
748 cortex inactivation in the monkey. Neuron 42, 501–508.
749 Watson, R.T., Valenstein, E., Day, A., Heilman, K.M., 1994. Posterior neocortical
750 systems subserving awareness and neglect. Neglect associated with superior
751 temporal sulcus but not area 7 lesions. Arch. Neurol. 51, 1014–1021.
752 doi:10.1001/archneur.1994.00540220060015
753 Weddell, R.A., 2004. Subcortical modulation of spatial attention including evidence that
754 the Sprague effect extends to man. Brain and Cognition 55, 497–506.
755 doi:10.1016/j.bandc.2004.02.075
756 Wilke, M., Kagan, I., Andersen, R.A., 2012. Functional imaging reveals rapid
757 reorganization of cortical activity after parietal inactivation in monkeys. PNAS 109,
758 8274–8279. doi:10.1073/pnas.1204789109
759 Xiang, Q.-S., Ye, F.Q., 2007. Correction for geometric distortion and N/2 ghosting in EPI
760 by phase labeling for additional coordinate encoding (PLACE). Magn. Reson. Med.

761 57, 731–741. doi:10.1002/mrm.21187

762 Yeterian, E.H., Pandya, D.N., 1989. Thalamic connections of the cortex of the superior

763 temporal sulcus in the rhesus monkey. J. Comp. Neurol. 282, 80–97.

764 doi:10.1002/cne.902820107

765 Zénon, A., Krauzlis, R.J., 2012. Attention deficits without cortical neuronal deficits.

766 Nature 489, 434–437. doi:10.1038/nature11497

767

768

769

770

771

Figure Legends

Figure 1. Behavioral tasks and midbrain-induced neglect (SC inactivation)

A) In the Baseline task, a black square around the central fixation spot instructed the monkey to monitor the fixation stimulus and detect luminance-change during a delay period of 1 – 3 seconds.

B) In the Ignore task, a black square around the central fixation spot instructed the monkey to monitor the fixation stimulus in the presence of peripheral motion distractors and detect luminance-change during a delay period of 1 – 3 seconds. Independent of the fixation spot dimming, one of the motion stimuli changed direction which the monkey ignored as part of the task.

C) In the Attend task, a red square around the central fixation spot instructed the monkey to monitor both the peripheral motion stimuli and detect a possible motion direction-change that occurred in one of the motion stimuli during a delay period of 1 – 3 seconds. The central fixation spot did not dim during Attend condition. In all tasks, the monkey reported the relevant change by releasing the joystick within 0.8 s for a juice reward.

D) Timeline of an example SC inactivation session and imaging. The session began with reversible inactivation of SC outside the scanner. In the scanner, the monkey performed all three tasks presented in a block design during an imaging run that lasted 8 minutes (black bars). At the end of each imaging run, the monkey performed visual guided saccades to targets in the affected and unaffected visual fields (grey bars). An average of 14 imaging runs were collected in an inactivation session.

794 E) The visual field map shows the effect of SC inactivation on the peak velocity of the
795 saccades to targets in the visually guided saccade task (top panel). The blue region
796 indicates the affected part of the visual field. Black dots indicate the retinotopic position
797 of the saccade targets. The white circles indicate the positions of the motion stimuli in
798 the Ignore and Attend tasks. The time course of muscimol effect was measured in the
799 scanner using visual guided saccade task at the end of each imaging run (bottom
800 panel). Blue dots indicate the latencies of saccades to targets in the affected visual field
801 and green dots indicate the latencies of saccades to targets in the unaffected visual
802 field. μ and σ indicate mean and standard deviation respectively.
803 F) Performance in Attend task is shown for control (green), neglect (SC inactivation;
804 blue) and saline (black) sessions in both monkeys. % Hit rate for motion changes in the
805 affected visual field (y-axis) is plotted against % hit rate for motion changes in the
806 unaffected visual field (x-axis). Each data point represents a single session and error
807 bars indicate 95% CI.
808
809 **Figure 2. Cortical maps of attention-related modulation in control and neglect (SC**
810 **inactivation) sessions**
811 T-scores contrasting Attend and Ignore tasks were projected onto inflated cortical
812 surfaces of D99 in each monkey's native space along with anatomical boundaries (black
813 contours).
814 (A, B) Inflated cortical maps of t-scores show attention-related modulation in ipsilateral
815 (left) hemisphere of monkey # 1 during control (A) and neglect (B). The maps were

816 thresholded during control sessions (A) and the modulation for the same voxels is
817 shown during the neglect sessions (B).
818 (C, D) Same conventions as (A, B) but for monkey # 2.
819 See also Figure S1.
820
821 **Figure 3. Midbrain-induced neglect linked to aFST/IPa region**
822 (A, B) Inflated cortical maps of interaction term F-statistic show voxels whose
823 modulation was affected during neglect in the ipsilateral hemisphere of monkey # 1 (A)
824 and monkey # 2 (B). The effect during neglect is shown for the same voxels that
825 showed significant modulation during control sessions (Fig. 2A, 2C). The blue color
826 indicates voxels whose modulation was reduced the most during neglect and the green
827 colors indicate voxels with no reduction in modulation. The white contour indicates the
828 contiguous cluster of affected voxels in aFST/IPa region.
829 (C, D) Magnified versions of Fig. 4A and 4B highlighting the most affected mid-STS
830 aFST/IPa region during neglect in monkey # 1 (C) and monkey # 2 (D).
831 (E, F) Coronal slices show the anatomical locations of the affected aFST/IPa region in
832 monkey # 1 (E) and monkey # 2 (F). The white cross-hairs indicate the peaks of the
833 aFST/IPa ROI from Fig. 4A.
834 See also Figures S2, S3.
835
836 **Figure 4. Effect of midbrain-induced neglect (SC inactivation) on the attention-**
837 **related modulation in cortical ROIs**

838 (A – I) The name of the ROI is shown at the top-left of each row. Each row shows
839 coronal slices containing the peak of the ROI for both monkeys (Monkey # 1: Left
840 column; Monkey # 2: Right column). The coronal slices overlaid with attention-related
841 modulation during control and neglect (SC inactivation) sessions are shown next to
842 each other for comparison (as in Fig. 2). The location of the white cross-hair in each
843 coronal slice indicates the peak of the ROI in the hemisphere ipsilateral to the SC
844 inactivation site. Note that the peak of the ROI was identified based on the attention-
845 related modulation during control. The location of the coronal slice w.r.t the inter-aural
846 axis is shown on top of each coronal slice. Next to the coronal slices, mean BOLD time-
847 courses for the ipsilateral ROI are plotted as % change in BOLD on y-axis against
848 repetition time (TR) on the x-axis for the Attend (filled circles) and Ignore (open circles)
849 tasks performed during control (orange) and neglect (blue) sessions. TR = 0 on x-axis
850 indicates start of the block. The bar plot shows the attention-related modulation in the
851 ipsilateral ROI measured as d' during control (orange) and neglect (blue) sessions. For
852 comparison, the same measure is shown for the corresponding contralateral ROI during
853 control and neglect sessions. Error bars indicate bootstrapped 95% CI and ∗ indicates
854 statistical significance at 5% ($p < 0.05$). aFST refers to anterior part of anatomical area
855 FST. See also Figure S4.
856
857 **Figure 5. Effect in aFST/IPa region during neglect was not contingent on visual**
858 **motion**

859 (A, B) Same conventions as Fig. 1B, 1C except that peripheral motion stimuli were
860 replaced by white noise distractors and the motion-change event was replaced by a
861 brief (0.5 s) second-order orientation pulse.
862 C) Performance in the Attend task is shown for control (green) and neglect (blue)
863 sessions in monkey # 1. Hit rate (%) for orientation pulse in the affected visual field (y-
864 axis) is plotted against hit rate for orientation pulse in the unaffected visual field (x-axis).
865 Each data point represents a single session and error bars indicate 95% CI.
866 (D, E) Inflated cortical maps of t-scores contrasting the Attend (Fig. 5B) and Ignore (Fig.
867 5A) tasks show attention-related modulation in the ipsilateral (left) hemisphere of
868 monkey # 1 during control (D) and neglect (E) sessions. The black arrow points to the
869 modulation in aFST/IPa region during control (D). The maps were thresholded during
870 control sessions (D) and the modulation for the same voxels is shown during the neglect
871 sessions (E).
872 F) Magnified version of the inflated cortical map of the interaction term F-statistic shows
873 the changes in attention-related modulation during neglect in ipsilateral STS regions
874 including aFST/IPa of monkey # 1 in the second-order orientation task. The effect
875 during neglect is shown for the same voxels that showed significant modulation during
876 control sessions (Fig. 5D). The blue color indicates voxels whose modulation was
877 reduced the most during neglect and the green colors indicate voxels with no reduction
878 in modulation. The white contour indicates the aFST/IPa region affected during neglect
879 in the motion task and is the same as shown in Fig. 3C.

880 G) Coronal slice displays the anatomical location of affected aFST/IPa region in monkey
881 # 1 in the second-order orientation task. The white cross-hair indicates voxel with peak
882 attention-related modulation in aFST/IPa region during control.
883
884 **Figure 6. The same aFST/IPa region was affected during FEF-induced neglect**
885 A) Coronal section shows the localization of FEF in the anterior bank of arcuate sulcus
886 and illustrates two sample sites (red circles) at which electrical stimulation (70 ms train
887 duration, 350 Hz, biphasic pulses with duration of 0.3 ms, 40 μA) evoked saccadic eye
888 movements with directions and amplitudes (indicated by the trajectories in each of the
889 two corresponding panels) that depended on the location within the FEF. White stripes
890 in upper right of the MRI were produced by the contrast agent placed in the FEF
891 recording grid and the superimposed yellow line indicate the estimated electrode and
892 injectrode paths.
893 B) The visual field map shows the affected visual field (blue region) during FEF
894 inactivation. Same conventions as Fig. 1E (top panel).
895 (C, D) Inflated cortical maps of t-scores contrasting the Attend (Fig. 1C) and Ignore (Fig.
896 1B) tasks show attention-related modulation in the ipsilateral (right) hemisphere of
897 monkey # 2 during control (C) and neglect (D) sessions. The black arrow points to the
898 modulation in aFST/IPa region during control (C). The maps were thresholded during
899 control sessions (C) and the modulation for the same voxels is shown during the neglect
900 sessions (D).
901 E) Magnified version of the inflated cortical map of the interaction term F-statistic shows
902 the changes in attention-related modulation during FEF-induced neglect in ipsilateral

903 STS regions including aFST/IPa of monkey # 2 in the motion task. The effect during
904 neglect is shown for the same voxels that showed significant modulation during control
905 sessions (Fig. 6C). The blue color indicates voxels whose modulation was reduced the
906 most during neglect and the green colors indicate voxels with no reduction in
907 modulation. The white contour indicates the aFST/IPa region affected during midbrain-
908 induced neglect (SC inactivation) in motion task and is the same as shown in Fig. 3D.
909 F) Coronal slice shows the anatomical location of the affected aFST/IPa region during
910 FEF inactivation in monkey # 1. The white cross-hair indicates voxel with peak
911 attention-related modulation in aFST/IPa region during control sessions.
912
913
914
915

916 **Methods**

917 *Animals*

918 Two adult male rhesus monkeys (*Macaca mulatta*) weighing 7-9 kg participated
919 in this study. All experimental protocols were approved by the National Eye Institute
920 Animal Care and Use Committee and all procedures were performed in accordance with
921 the United States Public Health Service policy on the humane care and use of
922 laboratory animals. Under isoflurane and aseptic conditions, we surgically implanted
923 plastic head-posts and electrophysiology chambers to access the SC and FEF. The SC
924 chamber was angled 38º to the posterior of vertical and directed at the midline, 15 mm
925 above and 1 mm posterior to the interaural line. The FEF chamber was angled 30º
926 lateral of vertical and aimed at a point 18 mm lateral from the midline, 25 mm anterior to
927 the interaural line.

928

929 *Experimental apparatus*

930 Monkeys were seated and head-fixed in a custom-built MR-safe chair with a
931 joystick attached inside the chair. Before each imaging session, monkeys performed a
932 visual guided saccade task inside a darkened booth. The saccade task was controlled
933 using a modified version of PLDAPS (Eastman and Huk, 2012). Animals viewed visual
934 stimuli from a distance of 48 cm that were displayed at 1920 x 1200 resolution (~ 60° x
935 38°) and 100Hz frame-rate on a VIEWPixx display (VPixx Technologies, Saint-Bruno,
936 QC Canada), controlled by a mid-2010 Mac Pro (Apple Inc., Cupertino, CA) running
937 MATLAB (The Mathworks, Natick, MA) with the Psychophysics Toolbox extensions
938 (Brainard, 1997; Kleiner et al., 2007; Pelli, 1997). Eye position was recorded using an

939 EyeLink 1000 infrared eye-tracking system (SR Research Ltd., Ottowa, Ontario,
940 Canada).
941 During each imaging session, monkeys performed attention tasks and visual
942 guided saccade task inside the vertical scanner. Stimuli were back projected on to a
943 screen placed inside the bore of the vertical scanner using an Epson projector
944 controlled by a Windows 2007 machine running MATLAB R2012b (The Mathworks) with
945 the psychophysics toolbox extensions (Brainard, 1997). The timing of the stimuli and
946 events were controlled by a QNX system running QPCS. Monkey viewed the screen
947 through a mirror placed in front at a 45° angle. The total viewing distance of the screen
948 was 53 cm. Eye movements were acquired and monitored in the scanner using an
949 iView system (Version 2.4, SensoMotoric Instruments). Eye signal was calibrated at the
950 beginning of each session. Joystick presses and releases were detected by disruption
951 of an optic-fiber transmission using a custom-built device. Joystick was calibrated once
952 at the beginning of the experiments.
953
954
955 *Attention tasks: Motion-change detection*
956 In the scanner, both monkeys performed three behavioral tasks: Baseline, Ignore
957 and Attend. In all tasks, monkeys initiated the trial by holding the joystick down and
958 fixating the central fixation spot with a colored central cue on a grey background.
959 Monkeys fixated for the entire duration of the trial with in a 2° fixation window. The color
960 of the central cue indicated the trial condition. In Baseline and Ignore trials, the color of
961 the central cue was black (Fig. 1A, 1B) and the relevant stimulus was the fixation

962 stimulus. In Attend trials, the color of the central cue was red (Fig. 1C) and the relevant
963 stimulus was the peripheral motion stimulus. The sequence of events in three different
964 trial conditions are as follows.

965 In Baseline trials, following 0.5 s of fixation, the luminance of the fixation spot
966 decreased during a variable delay of 1 – 3 s on the 65% of the trials. Monkeys reported
967 the luminance change by releasing the joystick within 0.3 - 0.8 s to get a juice reward
968 (Fig. 1A). A total of 8401 trails (4433 in Monkey #1 and 3968 in Monkey #2) were
969 collected during control and 7484 trails (3667 in Monkey #1 and 3817 in Monkey #2)
970 were collected during SC inactivation in both monkeys. We also collected 4446 trials
971 during saline injection in monkey #1.

972 In Ignore trials, following 0.5 s of fixation, two random dot motion stimuli were
973 presented on either side of fixation at 8° eccentricity (radius) and 10° above horizontal
974 meridian (azimuth). During the variable delay of 1 – 3 s, the luminance of the fixation
975 spot decreased on 65% of the trials. Independent of the fixation luminance change, one
976 of the peripheral motion stimulus changed direction during the variable delay of 1 – 3 s
977 on the 65% of the trials. Monkeys ignored the motion direction change and reported the
978 luminance change by releasing the joystick within 0.3 - 0.8 s to get a juice reward (Fig.
979 1C). If the monkeys released the joystick for a motion direction change, the trial was
980 aborted. A total of 9139 trails (4912 in Monkey #1 and 4227 in Monkey #2) were
981 collected during control and 8240 trails (4083 in Monkey #1 and 4157 in Monkey #2)
982 were collected during SC inactivation in both monkeys. We also collected 4913 trials
983 during saline injection in monkey #1.

984 In Attend trials, following 0.5 s of fixation, two random dot motion stimuli were
985 presented at the same stimulus location as in Ignore trials. One of the peripheral motion
986 stimulus changed direction during the variable delay of 1 – 3 s on the 65% of the trials.
987 Monkeys reported the motion-direction change by releasing the joystick within 0.3 - 0.8
988 s to get a juice reward (Fig. 1E). There was no fixation luminance change in Attend
989 trials. A total of 8672 trails (4765 in Monkey #1 and 3907 in Monkey #2) were collected
990 during control and 7742 trails (4026 in Monkey #1 and 3716 in Monkey #2) were
991 collected during SC inactivation in both monkeys. We also collected 4794 trials during
992 saline injection in monkey #1.
993 In all tasks, 35% of the trials were catch trials and monkeys hold the joystick
994 down to get a juice reward.
995
996 *Random dot motion stimuli*
997 The random dot motion stimuli were circular patches of moving dots, with the
998 direction of motion of each dot drawn from a normal distribution with a mean value
999 (defined as the patch motion direction) at 30° above horizontal and a 16° standard
1000 deviation. The lifetime (10 frames, 100 ms), density (25 dots/^{o2}/s), and speed of the dots
1001 (15 ^{o}/s) were held constant. The radius of the aperture was set to 3°. Luminance of each
1002 moving dot in the motion patches was 50 cd/m^2. The change in direction of motion (Δ)
1003 was 1 ± 0.25 standard deviations for both monkeys across sessions.
1004
1005 *Fixation spot stimulus*

1006 The size of the fixation spot was 0.23° and the size of the central cue was 0.35°.
1007 The background luminance of the screen was 14 cd/m^2 and the luminance of the
1008 fixation spot was 50 cd/m^2. The luminance change in fixation spot during Baseline and
1009 FA trials was 1-2 cd/m^2 across sessions for both monkeys.
1010
1011 *Attention tasks: Orientation-pulse detection*
1012 In addition to the motion-change detection task, monkey # 1 also performed a
1013 version of the attention tasks with orientation pulse stimuli instead of the random dot
1014 motion stimuli. The sequence of events in all three conditions (Baseline, Ignore, Attend)
1015 was kept the same as the motion-change detection version of the task. The onset of the
1016 motion stimuli was replaced with the onset of white noise stimuli, and the motion-
1017 direction change was replaced with a 0.5 s second-order orientation pulse (Fig. 5A, 5B).
1018 In the Attend condition, the monkey reported the orientation pulse by releasing the
1019 joystick within 0.3 - 0.8 s to get a juice reward (Fig. 5A), whereas in the Ignore condition,
1020 monkey ignored the orientation pulse and reported the luminance change in the fixation
1021 spot by releasing the joystick within 0.3 - 0.8 s to get a juice reward (Fig. 5B). In the
1022 Attend condition, a total of 3700 trails were collected during control and 2680 trails were
1023 collected during SC inactivation. In the Ignore condition, a total of 3752 trails were
1024 collected during control and 2698 trails were collected during SC inactivation.
1025 The second-order orientation stimulus was generated by briefly (0.5 s)
1026 modulating the contrast of a white noise stimulus with a 2-dimensional sinusoid. The
1027 noise stimulus was 6^0 in diameter and consisted of checks each the size of a pixel with
1028 luminance values ranging from 8 – 84 cd/m^2, and the 2-dimensional sinusoid had a

1029 spatial frequency of 0.7 cycles/deg, and its orientation was 90^0. We refer to this as a
1030 second-order orientation stimulus, because the oriented grating briefly visible in the
1031 stimulus was due to the local differences in contrast, not luminance differences. The
1032 mean luminance (38 cd/m^2) of the stimulus was constant throughout its presentation
1033 and was the same across every band in the oriented grating.
1034
1035 *Block Design*
1036 Baseline, Ignore and Attend tasks were presented in a block design as shown in
1037 Fig. 1D. Each run started with a Baseline block which lasted for 10 s and was presented
1038 in every alternate block thereafter. Ignore and Attend blocks lasted for 20 s and were
1039 presented randomly between Baseline blocks. The number of Ignore and Attend blocks
1040 were balanced in a given run. Each run lasted 480s.
1041
1042 *Electrophysiology*
1043 Locations for muscimol injections in the SC and FEF were identified by single-
1044 unit recording and electrical microstimulation. Single-unit activity was recorded using
1045 tungsten in glass-coated electrodes with impedances of 1-2 MOhm (Alpha Omega Co.,
1046 Inc., Alpharetta, GA). Electrode position was controlled with a Narishige microdrive. The
1047 electrical signal was amplified and recorded online using the OmniPlex system (Plexon
1048 Inc., Dallas, Texas). Response fields and saccade-related movement fields were
1049 mapped by having the monkey perform the visually guided saccade task; we confirmed
1050 saccade-related activity consistent with the known activity patterns in the FEF or SC.
1051 Electrical microstimulation was also applied (70 ms train duration, 350 Hz, biphasic

1052 pulses with duration of 0.25 ms) to evoke saccades with currents (40 μA in FEF; 20 μA
1053 in SC) confirming that we were in the FEF or intermediate layers in SC (Bruce and
1054 Goldberg, 1985; Robinson, 1972). All candidate sites were first identified by neuronal
1055 recordings and electrical stimulation prior to the muscimol inactivation experiment; in
1056 some cases, the FEF or SC site was verified immediately prior to muscimol injection
1057 using the electrode placed within the injection cannula (Lovejoy and Krauzlis, 2010).
1058
1059 *Muscimol infusion*
1060 Reversible inactivation of the intermediate layers of the SC (n = 27; monkey #1:
1061 19, monkey #2: 8) and FEF (n = 7; monkey #2) were done by injecting muscimol (5
1062 mg/ml). The amount of muscimol injected ranged from 0.3 – 0.5 μl in SC and 1 – 2 μl in
1063 FEF. Infusion was done using a custom-made apparatus modified from (Chen et al.,
1064 2001), with an injection pump at a rate of 0.5 μl in 10 mins. For saline controls in SC,
1065 0.3 – 0.5 μl of saline was injected at the same location in the intermediate layers of the
1066 SC.
1067
1068 *Visually guided saccade task and mapping of affected visual field*
1069 In the saccade task, each trial started with the monkeys fixating a small square
1070 stimulus (0.23^{o} wide, 50 cd/m^{2}) placed at the center of the visual display. After 500 ms
1071 of fixation, a second target (0.23^{o} wide, 50 cd/m^{2}) was presented at some other location
1072 in the visual display. Monkeys were required to maintain fixation until the central fixation
1073 stimulus was turned off, 1-2 seconds after the onset of the peripheral target. At that
1074 point, the monkeys should make a saccade to the second, peripheral target and fixate it

1075 for at least 500 ms in order to receive a reward. The eye position data were used to
1076 detect saccades and quantify saccade metrics offline using methods described
1077 previously (Madelain et al., 2005).

1078 Before imaging, monkeys performed the saccade task outside the scanner and
1079 the location of the second target was systematically varied every trial in order to quantify
1080 the metrics of saccades to targets across the visual field. We quantified the impairments
1081 in saccade metrics during SC or FEF inactivation by measuring the difference in the
1082 peak velocity for saccades made to targets at different locations in the visual field before
1083 and during inactivation. The target locations where the peak velocities of the saccades
1084 were impaired identified the affected visual field (Fig. 1E, 6B). Data were collected
1085 beginning 30 minutes after the end of the muscimol infusion.

1086 Inside the scanner, monkeys performed the saccade task every 8 minutes and
1087 the location of the second target was alternated each trial between contralateral and
1088 ipsilateral stimulus locations (radius: 8°; azimuth: 10°). The time course of muscimol
1089 effect was measured as a difference in the saccade latency to targets in the
1090 contralateral affected visual field compared to targets in the ipsilateral unaffected visual
1091 field (Fig. 1E). We measured the impairment on the saccade latency instead of peak
1092 velocity in the scanner because, the low sampling frequency of the eye tracker in the
1093 scanner limited the accurate measurement of peak velocities.

1094

1095 *fMRI data collection*

1096 Anatomical and functional images were collected in a vertical magnet (4.7T, 60
1097 cm vertical bore; Bruker Biospec) equipped with a Bruker S380 gradient coil. EPI

volumes were acquired using a custom built transmit and 4-channel receive RF coil system (Rapid MR International). In each run, we collected 192 whole-brain EPI volumes at an isotropic voxel resolution of 1.5 mm and at a TR of 2.5 s.

fMRI Analysis

Preprocessing of the fMRI data was done using AFNI/SUMA software package (Cox, 1996). Raw images were converted to AFNI data format. EPI volumes in each run were slice-time corrected using *3dTshift*, followed by correction for static magnetic field inhomogeneities using the *PLACE* algorithm (Xiang and Ye, 2007). All EPI volumes were motion-corrected using *3dvolreg* and were registered to the session anatomical using *3dAllineate*. To combine EPI data across multiple sessions for a given animal, all sessions for a given animal were registered to a template session. A high resolution anatomical of each monkey was registered to the corresponding template session anatomical to overlay functional results in monkey's native space. To overlay D99 atlas boundaries on the functional results, D99 anatomical in AFNI was registered to each monkey's native space (Reveley et al., 2017). Surface maps were generated for D99 anatomical in each monkey's native space using CARET from a white matter segmentation mask (Van Essen et al., 2001). Surface maps of D99 in each monkey's native space were viewed in SUMA overlaid with anatomical boundaries and functional results.

Functional maps of attention-related modulation

1120 To identify voxels that were modulated by attention we performed a GLM
1121 analysis using *3dDeconvolve* in AFNI. Attend and Ignore conditions were included as
1122 regressors of interest and Baseline condition, motion correction parameters were
1123 included as regressors of no interest (baseline model). To control for the effects caused
1124 by any differences during Attend and Ignore blocks in blinks (Wilcoxon rank sum test, p
1125 $= 0.007$ (Monkey # 1), $p = 0.99$ (Monkey # 2)), saccadic eye movements within the
1126 fixation window (Wilcoxon rank sum test, $p < 0.0001$ (Monkey # 1), $p < 0.0001$ (Monkey
1127 # 2)), rewards (Wilcoxon rank sum test, $p < 0.0001$ (Monkey # 1), $p < 0.0001$ (Monkey #
1128 2)) and joystick movements (Wilcoxon rank sum test, $p = 0.79$ (Monkey # 1), $p = 0.53$
1129 (Monkey # 2)), we included these factors as part of the regression model. Reward
1130 times, joystick event times (press and release), blink times and saccade times (left and
1131 right) were convolved with the hemodynamic impulse response function and were
1132 included as part of the baseline model. In the blocks of all three conditions for both
1133 monkeys, the median duration of fixation was above 85% of the block duration.
1134 Saccades within the fixation window (magnitude less than 1°) were detected using
1135 previously described methods (Madelain et al., 2005). T-scores contrasting Attend and
1136 Ignore conditions were projected on to the inflated maps to show voxels modulated by
1137 attention. All functional maps were thresholded (t-score > 5.02) to correct for multiple
1138 comparisons ($p<0.05$, Bonferroni correction).
1139
1140 *Functional regions of interest and attention-related modulation*
1141 Functional regions of interest (ROIs) were identified based on the local maxima
1142 of the attention-related modulation map from the control sessions for each hemisphere

using *3dExtrema* in AFNI. The BOLD time-course for each Attend or Ignore block was computed as a % change in BOLD relative to the BOLD in Baseline block preceding it. For each ROI, an average time-course was constructed by pooling time-courses of all voxels within a 2mm radius around the local maxima across all blocks from all sessions. D-prime was computed for each ROI as a measure of attention-related modulation from the Attend and Ignore distributions of BOLD values taken from the TRs 2 – 8 of each block. Attend and Ignore distributions were constructed by pooling BOLD values across voxels in a given ROI and across blocks from different sessions. The mean and variance of the Attend (μ_A, σ_A^2) and Ignore (μ_I, σ_I^2) distributions were used to compute d-prime (d') following equation 1. The source of the variance in the Attend and Ignore distributions came from pooling BOLD values across blocks, sessions and voxels in a given ROI.

$$d' = (\mu_A - \mu_I)/(\sqrt{1/2(\sigma_A^2 + \sigma_I^2)}) \qquad \text{Equation 1}$$

Voxel-wise ANOVA

For each voxel, we performed ANOVA with two factors and two levels each – covert attention (Attend and Ignore conditions) and neglect (control and inactivation). The 2x2 factorial design for each voxel was based on the BOLD values taken from the TRs 2 – 8 of Attend and Ignore time courses extracted from the control and neglect sessions. F-statistic of the interaction term was projected onto the inflated maps to show the effect of inactivation on attention-related modulation. For every voxel, the sign of the difference in attention-related modulation between neglect and control

($d'_{Neglect} - d'_{Control}$) was added to the F-statistic of the interaction term to differentiate the decrease in modulation from increase in modulation.

Stimulus mapping experiment

To identify voxels responding to foveal and peripheral stimuli locations, a flickering checker board stimulus (4 Hz) that had concentric rings of 2° width spanning up to 12° eccentricity was used. In foveal visual stimulation blocks, the checker board stimulus was masked everywhere except for the central 2° radius. In peripheral visual stimulation blocks, the checker board stimulus was masked everywhere except for the two eccentric stimulus locations used in the attention tasks. The foveal and peripheral stimulation blocks (20 s duration) were interleaved with fixation blocks (10 s duration). A total of 258 runs (150 in Monkey #1; 108 in Monkey # 2) were collected in both monkeys across 13 sessions. Functional maps showing peripheral and foveal voxels were created using the same methods as described for creating functional maps for the attention tasks.

Figure 1

A Baseline task

Fixate (1 - 3 s)

Detect dim (0.8 s)

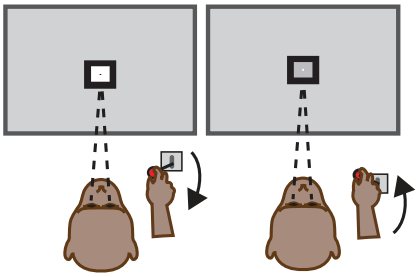

B Ignore task

Fixate (1 - 3 s)

Detect dim (0.8 s)

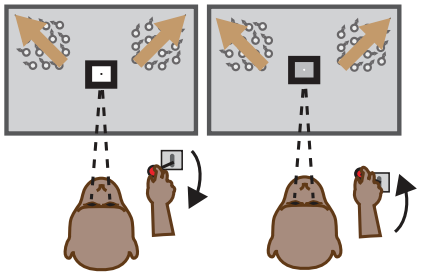

C Attend task

Fixate (1 - 3 s)

Detect motion Δ (0.8 s)

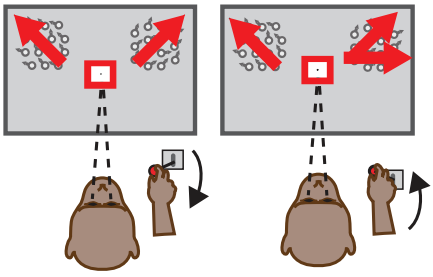

D SC inactivation and imaging

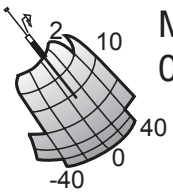

Muscimol 0.3 - 0.5 µl

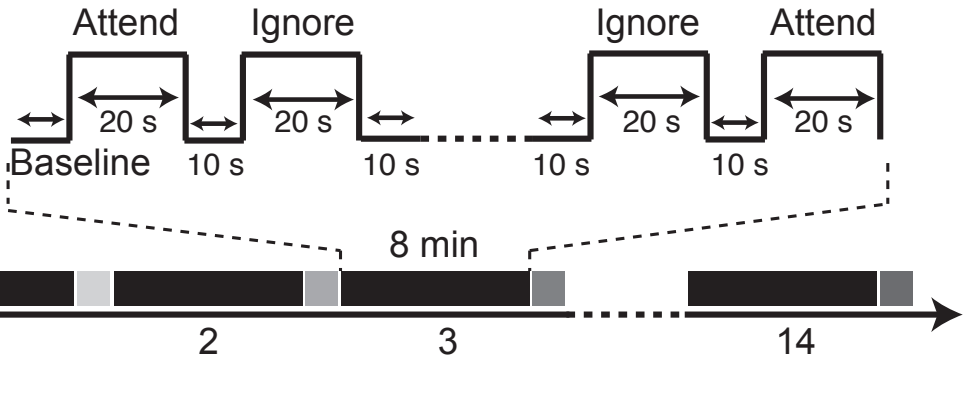

E Saccade deficits

Visual field map

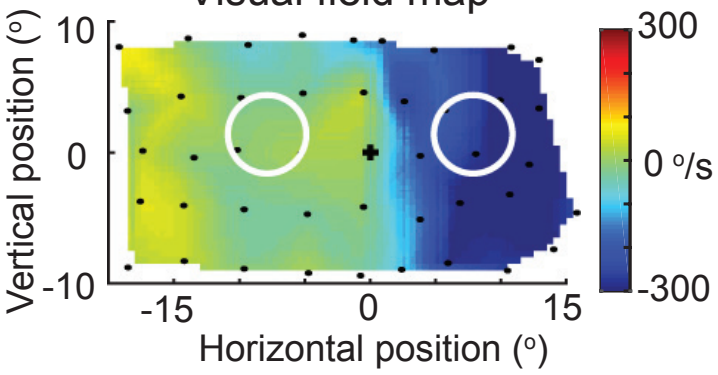

Time course

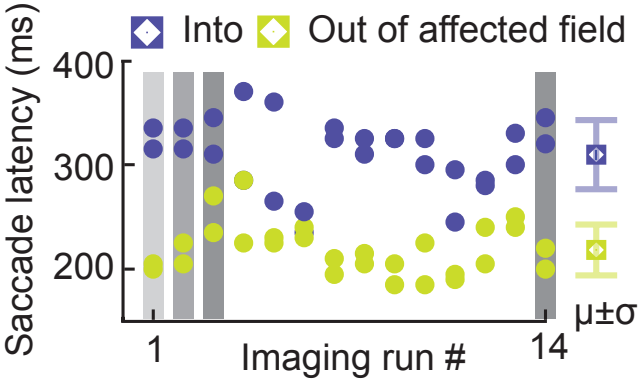

F Attention deficits

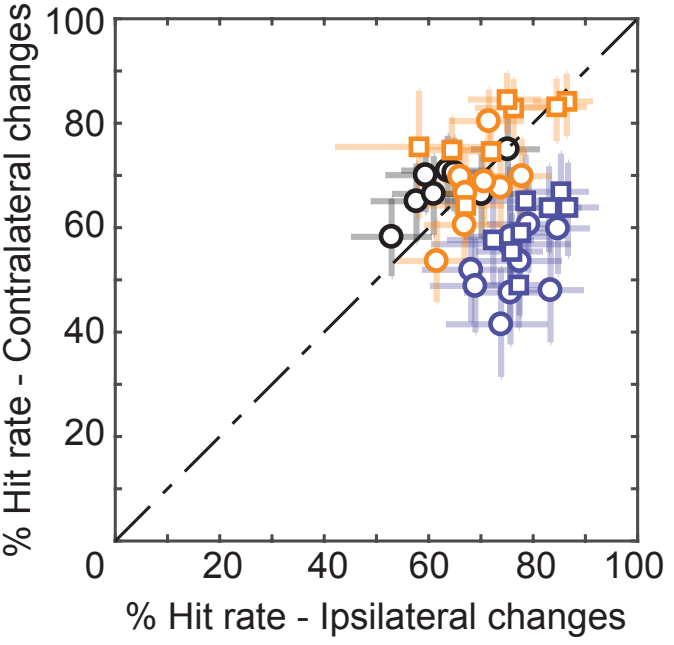

Control

Neglect

Saline

Subject # 1

Subject # 2

Figure 2

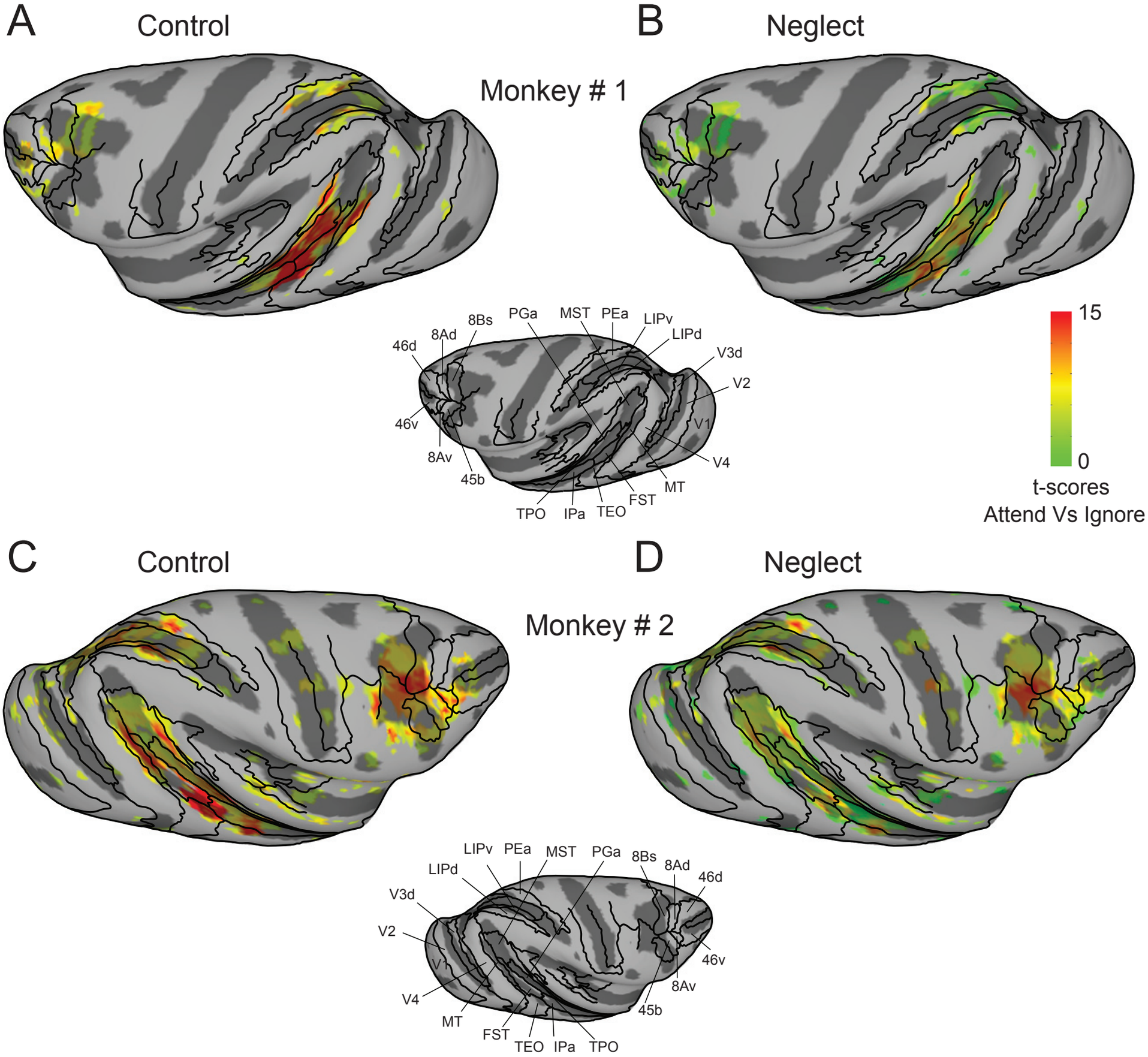
A
Control
B
Neglect
Monkey # 1
46d
8Ad
8Bs
PGa
MST
PEa
LIPv
LIPd
V3d
V2
V1
V4
MT
FST
TEO
IPa
TPO
45b
8Av
46v
15
0
t-scores
Attend Vs Ignore
C
Control
D
Neglect
Monkey # 2
LIPv
PEa
MST
PGa
8Bs
8Ad
46d
LIPd
V3d
V2
V1
V4
MT
FST
TEO
IPa
TPO
45b
8Av
46v

Figure 3

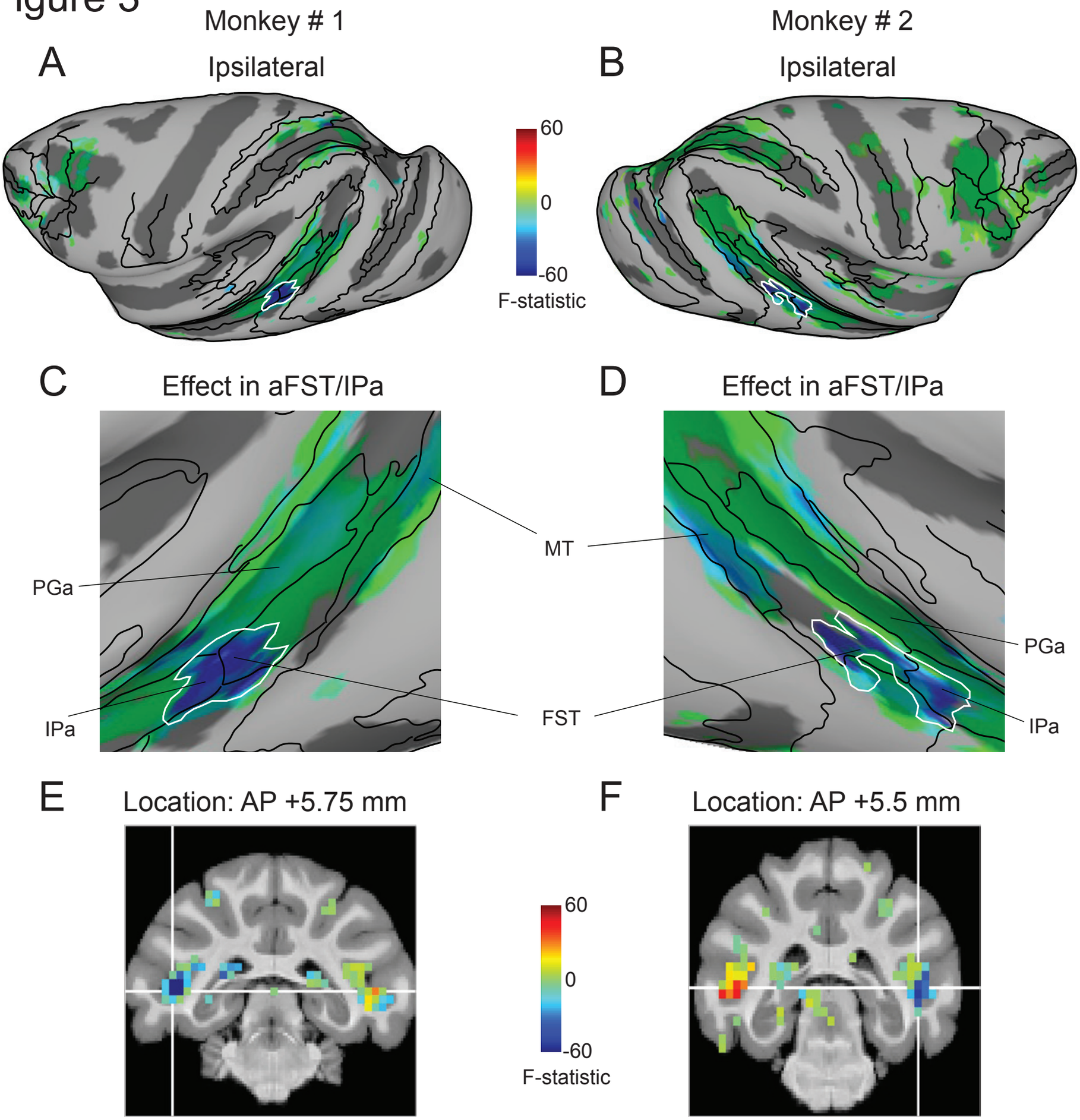
Monkey # 1
A
Ipsilateral
Monkey # 2
B
Ipsilateral
60
0
-60
F-statistic
C
Effect in aFST/IPa
D
Effect in aFST/IPa
MT
PGa
FST
IPa
PGa
IPa
E
Location: AP +5.75 mm
F
Location: AP +5.5 mm
60
0
-60
F-statistic

Figure 4

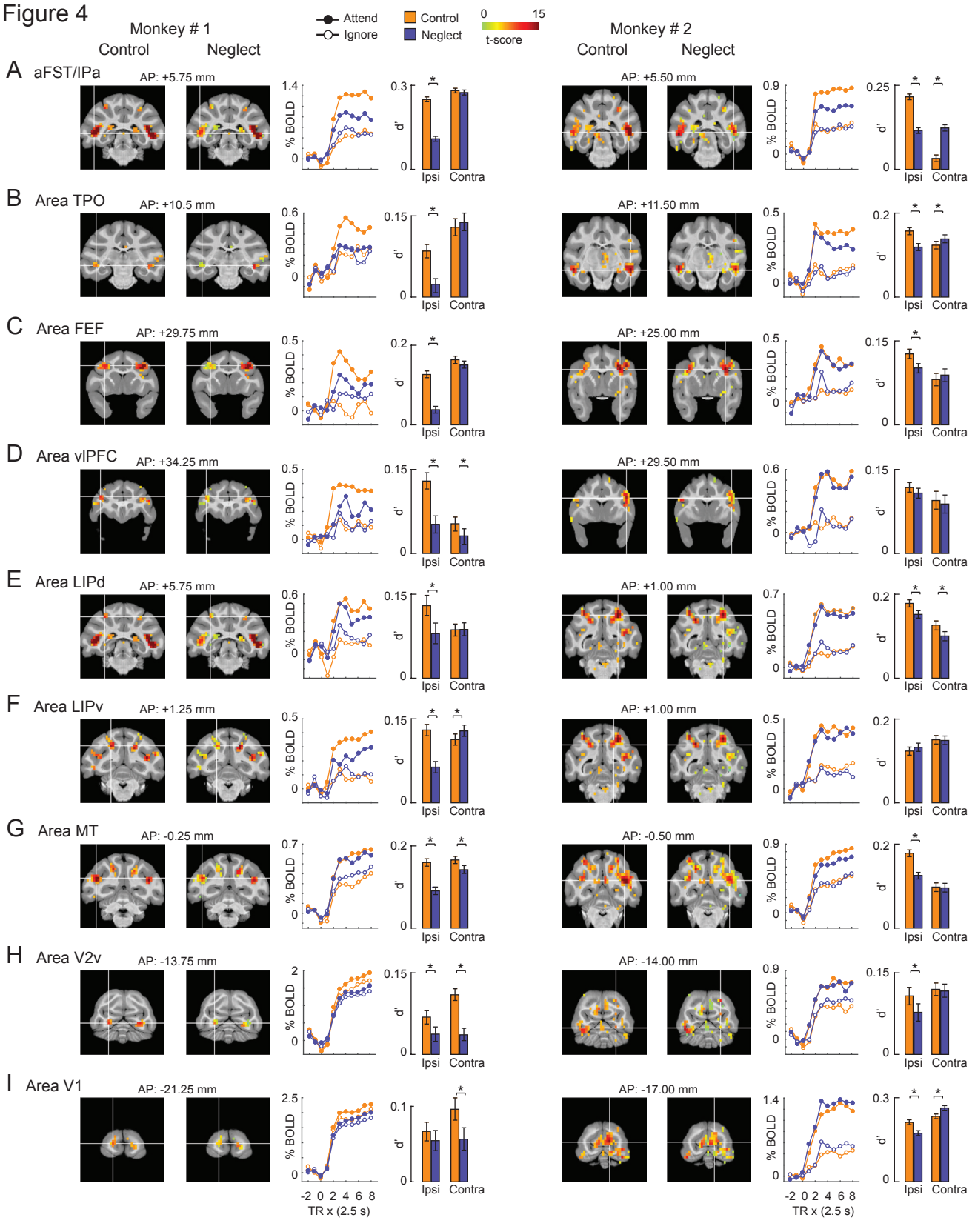
Monkey # 1
Control
Neglect
Attend
Ignore
Control
Neglect
0
15
t-score
Monkey # 2
Control
Neglect
A aFST/IPa
AP: +5.75 mm
AP: +5.50 mm
B Area TPO
AP: +10.5 mm
AP: +11.50 mm
C Area FEF
AP: +29.75 mm
AP: +25.00 mm
D Area vlPFC
AP: +34.25 mm
AP: +29.50 mm
E Area LIPd
AP: +5.75 mm
AP: +1.00 mm
F Area LIPv
AP: +1.25 mm
AP: +1.00 mm
G Area MT
AP: -0.25 mm
AP: -0.50 mm
H Area V2v
AP: -13.75 mm
AP: -14.00 mm
I Area V1
AP: -21.25 mm
AP: -17.00 mm
% BOLD
d'
Ipsi
Contra
-2 0 2 4 6 8
TR x (2.5 s)

Figure 5

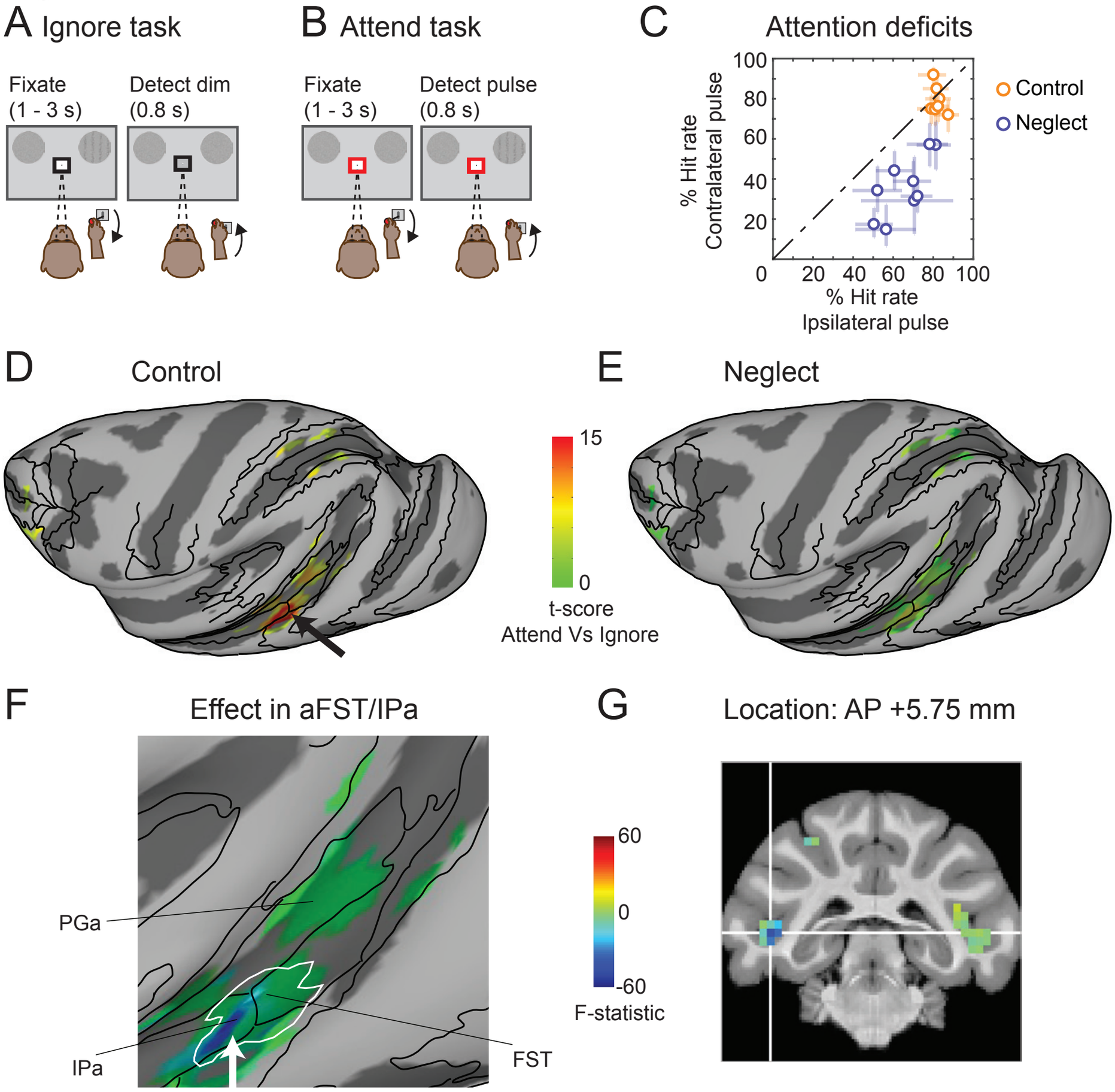
A Ignore task
Fixate
(1 - 3 s)
Detect dim
(0.8 s)
B Attend task
Fixate
(1 - 3 s)
Detect pulse
(0.8 s)
C
Attention deficits
% Hit rate
Contralateral pulse
% Hit rate
Ipsilateral pulse
0
20
40
60
80
100
Control
Neglect
D
Control
E
Neglect
15
0
t-score
Attend Vs Ignore
F
Effect in aFST/IPa
PGa
IPa
FST
G
Location: AP +5.75 mm
60
0
-60
F-statistic

Figure 6

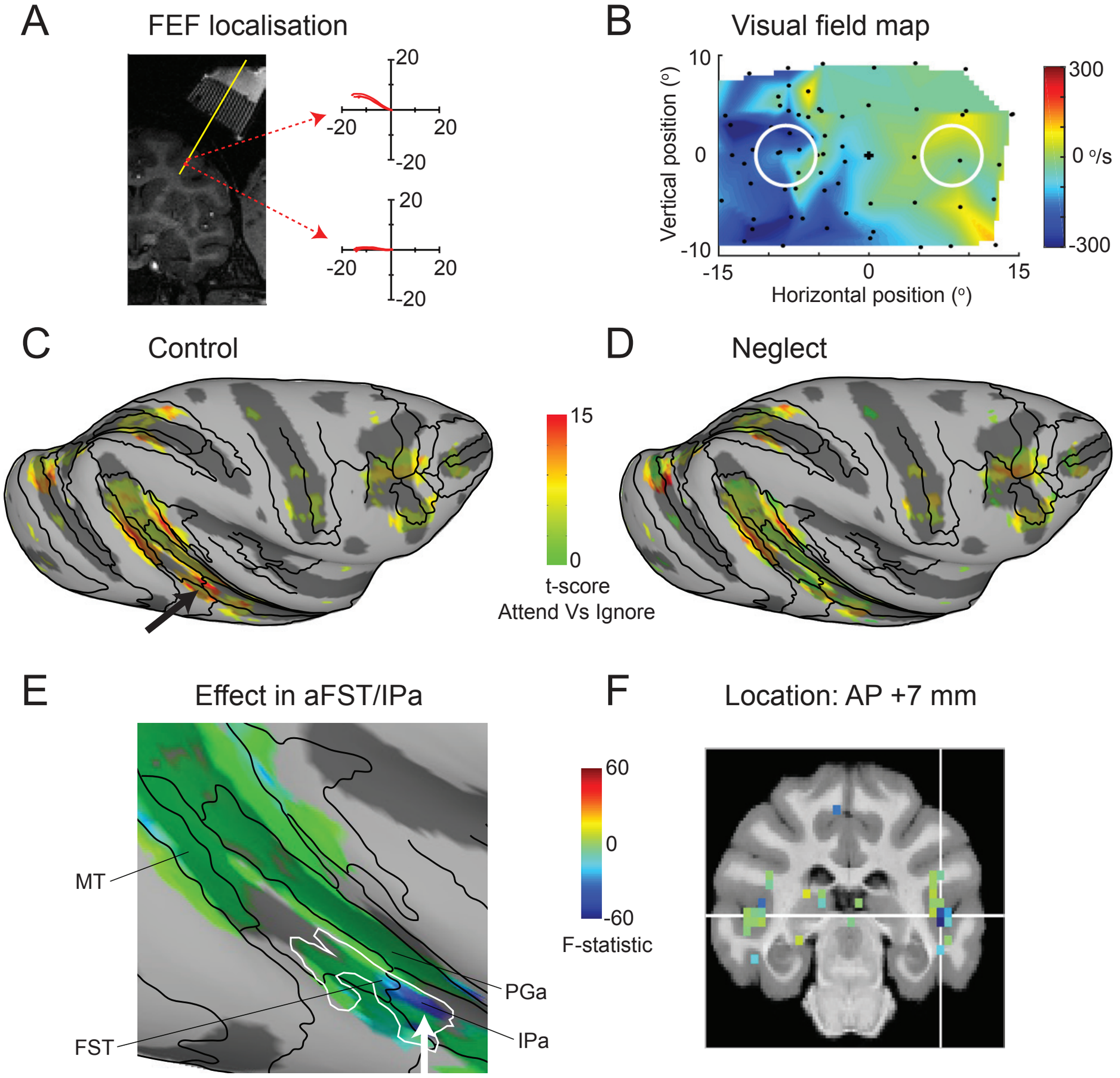
A
FEF localisation
20
-20
20
-20
20
-20
20
-20
B
Visual field map
10
0
-10
-15
0
15
Vertical position (°)
Horizontal position (°)
300
0 °/s
-300
C
Control
D
Neglect
15
0
t-score
Attend Vs Ignore
E
Effect in aFST/IPa
MT
FST
PGa
IPa
60
0
-60
F-statistic
F
Location: AP +7 mm